# AN INVESTIGATION OF THE ROLE OF SECOND PHASE PARTICLES IN THE DESIGN OF ULTRA HIGH STRENGTH STEELS OF IMPROVED TOUGHNESS

FINAL REPORT

W. M. Garrison, Jr.

Carnegie Mellon

(2)

# AN INVESTIGATION OF THE ROLE OF SECOND PHASE PARTICLES IN THE DESIGN OF ULTRA HIGH STRENGTH STEELS OF IMPROVED TOUGHNESS

FINAL REPORT

W. M. Garrison, Jr.
June 15, 1990

U.S. ARMY RESEARCH OFFICE

DAAL03-86-K-0124

Department of Metallurgical Engineering and Materials Science

CARNEGIE MELLON UNIVERSITY

Pittsburgh, PA 15213

UNCLASSIFIED
SECURITY CLASSIFICATION OF THIS PAGE

MASTER COPY - FOR REPRODUCTION PURPOSES

# REPORT DOCUMENTATION PAGE

| | |
|---|---|
| 1a. REPORT SECURITY CLASSIFICATION<br>Unclassified | 1b. RESTRICTIVE MARKINGS |
| 2a. SECURITY CLASSIFICATION AUTHORITY | 3. DISTRIBUTION/AVAILABILITY OF REPORT<br>Approved for public release; distribution unlimited. |
| 2b. DECLASSIFICATION/DOWNGRADING SCHEDULE | |
| 4. PERFORMING ORGANIZATION REPORT NUMBER(S)<br>1-50129 | 5. MONITORING ORGANIZATION REPORT NUMBER(S)<br>ARO 23261.10-MS |
| 6a. NAME OF PERFORMING ORGANIZATION<br>Carnegie Mellon University<br>6b. OFFICE SYMBOL (If applicable) | 7a. NAME OF MONITORING ORGANIZATION<br>U. S. Army Research Office |
| 6c. ADDRESS (City, State, and ZIP Code)<br>5000 Forbes Avenue<br>Pittsburgh, PA 15213 | 7b. ADDRESS (City, State, and ZIP Code)<br>P. O. Box 12211<br>Research Triangle Park, NC 27709-2211 |
| 8a. NAME OF FUNDING/SPONSORING ORGANIZATION<br>U. S. Army Research Office<br>8b. OFFICE SYMBOL (If applicable) | 9. PROCUREMENT INSTRUMENT IDENTIFICATION NUMBER<br>DAAL03-86-K-0124 |
| 8c. ADDRESS (City, State, and ZIP Code)<br>P. O. Box 12211<br>Research Triangle Park, NC 27709-2211 | 10. SOURCE OF FUNDING NUMBERS<br>PROGRAM ELEMENT NO. / PROJECT NO. / TASK NO. / WORK UNIT ACCESSION NO. |
| 11. TITLE (Include Security Classification)<br>An Investigation of the Role of Second Phase Particles in the Design of Ultra High Strength Steels of Improved Toughness | |
| 12. PERSONAL AUTHOR(S)<br>W. M. Garrison, Jr. | |
| 13a. TYPE OF REPORT<br>13b. TIME COVERED FROM 7/7/86 TO 6/1/90 | 14. DATE OF REPORT (Year, Month, Day)<br>1990, June 20 |
| 15. PAGE COUNT<br>51 | |
| 16. SUPPLEMENTARY NOTATION<br>The view, opinions and/or findings contained in this report are those of the author(s) and should not be construed as an official Department of the Army position, policy, or decision, unless so designated by other documentation. | |

| 17. COSATI CODES | | | 18. SUBJECT TERMS (Continue on reverse if necessary and identify by block number) |
|---|---|---|---|
| FIELD | GROUP | SUB-GROUP | |
| | | | |
| | | | |


19. ABSTRACT (Continue on reverse if necessary and identify by block number)

In this report are summarized work carried out as part of a research program designed to improve the upper shelf fracture toughness of ultra high strength steels and to gain further understanding of the processes associated with the fracture of these materials and how these processes are related to microstructure. The results emphasized are: (a) blunting behavior and its effects on toughness, (b) the effects of inclusion spacing at constant inclusion volume fraction on toughness, (c) observations on the effects of carbides and nitrides on toughness, (d) grain size effects and (e) studies of void nucleation at inclusions and the effects on toughness of gettering sulfur as particles rich in Ti, C, and S rather than as manganese sulfides. Our blunting studies indicate that blunting to vertices, although it is associated with low work hardening, appears to result in higher levels of toughness than smooth blunting. The results show that increasing inclusion spacing at constant inclusion volume fraction results in improvements in toughness until the inclusion spacing approaches some critical value; once the inclusion spacing exceeds that value the toughness is independent of particle spacing. It is suggested that grain size effects and particle spacing effects are interrelated. Finally, it is shown that replacing manganese sulfides by particles believed to be $Ti_2CS$ can result in doubling of the fracture toughness at constant inclusion volume fraction. This effect is attributed to the increased resistance of these particles to void nucleation.


| | |
|---|---|
| 20. DISTRIBUTION/AVAILABILITY OF ABSTRACT<br>☑ UNCLASSIFIED/UNLIMITED ☐ SAME AS RPT. ☐ DTIC USERS | 21. ABSTRACT SECURITY CLASSIFICATION<br>Unclassified |
| 22a. NAME OF RESPONSIBLE INDIVIDUAL | 22b. TELEPHONE (Include Area Code) / 22c. OFFICE SYMBOL |

DD FORM 1473, 84 MAR

83 APR edition may be used until exhausted.
All other editions are obsolete.

SECURITY CLASSIFICATION OF THIS PAGE
UNCLASSIFIED

# AN INVESTIGATION OF THE ROLE OF SECOND PHASE PARTICLES IN THE DESIGN OF ULTRA HIGH STRENGTH STEELS OF IMPROVED TOUGHNESS

FINAL REPORT

W. M. Garrison, Jr.
June 15, 1990

U.S. ARMY RESEARCH OFFICE

DAAL03-86-K-0124

Department of Metallurgical Engineering and Materials Science

CARNEGIE MELLON UNIVERSITY

Pittsburgh, PA 15213

# AN INVESTIGATION OF THE ROLE OF SECOND PHASE PARTICLES IN THE DESIGN OF ULTRA HIGH STRENGTH STEELS OF IMPROVED TOUGHNESS

W. M. Garrison, Jr.

Department of Metallurgical Engineering and Materials Science
CARNEGIE MELLON UNIVERSITY
Pittsburgh, PA 15213

## ABSTRACT

In this report are summarized work carried out as part of a research program designed to improve the upper shelf fracture toughness of ultra high strength steels and to gain further understanding of the processes associated with the fracture of these materials and how these processes are related to microstructure. The results emphasized are: (a) blunting behavior and its effects on toughness, (b) the effects of inclusion spacing at constant inclusion volume fraction on toughness, (c) observations on the effects of carbides and nitrides on toughness, (d) grain size effects and (e) studies of void nucleation at inclusions and the effects on toughness of gettering sulfur as particles rich in Ti, C, and S rather than as manganese sulfides. Our blunting studies indicate that blunting to vertices, although it is associated with low work hardening, appears to result in higher levels of toughness than smooth blunting. The results show that increasing inclusion spacing at constant inclusion volume fraction results in improvements in toughness until the inclusion spacing approaches some critical value; once the inclusion spacing exceeds that value the toughness is independent of particle spacing. It is suggested that grain size effects and particle spacing effects are interrelated. Finally, it is shown that replacing manganese sulfides by particles believed to be $Ti_2CS$ can result in doubling of the fracture toughness at constant inclusion volume fraction. This effect is attributed to the increased resistance of these particles to void nucleation.

TABLE OF CONTENTS


| | Page |
|---|---|
| Abstract | |
| A. Project Report | 3 |
| 1. Introduction | 3 |
| 2. Discussion of Results | 5 |
| 2.a. Blunting Studies | 6 |
| 2.b. Influence of Inclusion Spacing | 8 |
| 2.c. Influence of Undissolved Carbides | 11 |
| 2.d. Influence of Grain Size | 14 |
| 2.e. Void Nucleation Studies | 14 |
| 2.f. Microstructure and Fracture | 17 |
| 3. Summary of Accomplishments | |
| 3.a. Technical Highlights | 18 |
| 3.b. Degrees | 19 |
| 3.c. Papers | 19 |
| 3.d. Industrial Involvement | 20 |
| 3.e. Patent Application | 20 |
| 4. References | 21 |
| 5. Tables and Figures | 23 |

## A. Report

## 1. Introduction:

My original proposal to the Army Research Office began with the following statement:

"It is implicitly assumed in the approach to the design of ultra high strength steels that modifications of microstructure by changes in composition, heat treatment or both can be found which improve toughness. Certainly, this approach has enjoyed spectacular successes, notably the secondary hardening steels HY180 [1] and AF1410 [2]. The very high fracture toughnesses of these steels are due, at least in part, to the refinement of intra-lath carbide size achieved by replacing iron carbides by alloy carbides and employing large cobalt additions to reduce the alloy carbide size [1,3]. However, other than maintaining low inclusion volume fractions and the development of sulfide shape control [4-6], inclusions and their influence on toughness have largely been ignored in the design of new steels. This attitude has persisted despite interpretations of experimental studies [7,8] and the Rice and Johnson mode [9] which suggest for the ultra high strength steels that the crack tip opening displacement at fracture should scale as the inclusion spacing."

Thus it was proposed that improvements in toughness could be achieved by maximizing inclusion spacing by minimizing inclusion volume fraction and maximizing inclusion particle size. The first two goals of the proposed work were to develop processing techniques to control inclusion size and spacing and to exploit this microstructural control in assessing the influence of inclusion spacing and size on upper shelf fracture toughness.

As will be discussed, this work has been reasonably successful in controlling inclusion spacing in a manner which can be successfully applied with benefit to most steels. The inclusions in most steels are sulfides and oxides. Typically when the sulfides are manganese sulfides the average inclusion spacing is 2 to 3μm [10,11]. When the manganese sulfides are replaced by $La_2O_2S$ particles the particles are larger and have an average spacing of 7 to 15μm [3,12]. By so altering inclusion spacing the crack tip opening displacement at fracture ($\delta_{IC}$) increases by a factor of two or more [12]. However, recent work [13] has shown that at constant (and low) inclusion volume fractions $\delta_{IC}$ does not scale linearly with particle spacing as suggested by Rice and Johnson. Initially $\delta_{IC}$ increases almost linearly with particle spacing, $X_o$; however, the rate at which $\delta_{IC}$ increases with $X_o$ decreases with increasing $X_o$. In fact $\delta_{IC}$ seems to approach a limiting value which is believed to be determined by inclusion volume fraction, at least for a fixed fine scale microstructure [13]. Therefore, from the standpoint of improving toughness controlling

particle spacing is important but certainly less effective than anticipated. However, from a more fundamental point of view these results demonstrate that it is incorrect to assume, as is often done, that $\delta_{IC}$ scales as the particle spacing. While the improvements in toughness which can be achieved by maximizing the particle spacing are not as great as anticipated, our analysis, described in the background, suggests that reducing the inclusion volume fraction coupled with control of particle spacing will be very successful in enhancing toughness. Unfortunately, the inclusion volume fractions required to implement this approach are much too low to be achieved by even the best of current conventional commercial practices. Therefore a new approach to improving the fracture toughness of ultra high strength steels has been explored.

When changing inclusion type for otherwise constant microstructures, studies of void nucleation and growth have been carried out to ensure that inclusion spacing and size, and not void nucleation characteristics of the inclusions, were the only parameters being changed. It appears that void nucleation and growth at inclusions in steels are almost identical, whether the sulfides are manganese sulfides or $La_2O_2S$. In the course of this work on void nucleation and growth it was observed that it is possible to form inclusions rich in titanium, carbon and sulfur; these particles are believed to be titanium carbo-sulfides, $Ti_2CS$. As will be discussed these particles are extremely resistant to void nucleation and this characteristic seems to favor high toughnesses [14]. Specifically HY180 steel tempered at 510°C for 5 hours has a yield strength of about 1200 MPa and when the sulfides in the steel are manganese sulfides $\delta_{IC}$=130μm ($K_{IC}$ = 230 MPa$\sqrt{m}$); when the manganese sulfides are replaced by the same volume fraction of $Ti_2CS$ particles $\delta_{IC}$ = 706μm ($K_{IC}$ = 550 MPa$\sqrt{m}$). This control of void nucleation appears to be a promising approach to improving the toughness of many types of ultra-high strength steels and is a major thrust of the current work.

The approach taken to improving the fracture toughness of ultra high strength steels is to take advantage of the void nucleation characteristics of $Ti_2CS$ inclusions. By replacing manganese sulfides or $La_2O_2S$ particles by what are believed to be $Ti_2CS$ particles it may be possible to achieve exceptionally high toughnesses in many, but not all classes of steels. Certainly our initial work with HY180 is encouraging. However this approach raises issues of both fundamental and practical importance. First, that these particles are extremely resistant to void nucleation suggests high interfacial stresses [15,16,33] are needed to cause separation of the particle-matrix interface. It is most probable that this is due to strong chemical bonding between the particle and the matrix. At this time little is known about interfacial

structure and bonding at inclusions in steels. It is suggested such knowledge is important to our understanding of void nucleation at inclusions as well as at other particles. Second, it must be remembered that on introducing titanium there is potential for the formation of titanium carbides (or nitrides). Such particles at a given volume fraction and size may become much more detrimental to toughness as the strength increases [17]; also, the volume fraction and possibly the particle size will increase as the carbon content of the steel increases. Therefore, the extent to which the toughness of very high strength materials can be improved by replacing manganese sulfides by $Ti_2CS$ particles will probably depend on minimizing TiC formation by minimizing the titanium additions and by using appropriate processing and heat treatments. As a result, to implement this approach it will be necessary to determine the minimum amount of titanium required to ensure the formation of the $Ti_2CS$ inclusions. Finally it is emphasized that the processes involved in the fracture of ultra high strength steels are complex and isolating specific microstructural effects is essential to the success of this program. For example, studying the effects of $Ti_2CS$ inclusions on toughness will require careful assessment of void nucleation at these particles and the degree to which carbides and/or nitrides may influence toughness. Further, the benefits of resistance to void nucleation with respect to improving toughness probably vary with microstructure, even at constant flow stress.

In the background section work done over the past 2.5 years on the following topics will be reviewed. These include: (a) blunting behavior and its influence on toughness, (b) control of inclusion spacing and its influence of toughness, (c) observations on the influence of undissolved carbides and nitrides on toughness, (d) role of grain size, (e) studies of void nucleation at inclusions and the influence of void nucleation on toughness.

## 2. Discussion of Results:

The purpose of this section is to present and discuss further the important results from the last two and a half years. Certain work, such as the influence of austenitizing temperature on toughness and particle distributions and studies of sulfide coarsening will not be presented or completely presented; however, these studies have produced information which impact our current research. The five topics to be reviewed here are (a) blunting behavior, (b) control of inclusion spacing and the influence of inclusion spacing and volume fraction on toughness (c) observations on the influence of undissolved carbides and nitrides on toughness, (d) grain size effects, and (e) studies of the nucleation and subsequent growth of voids at inclusions and the influence of void nucleation on toughness. The section will conclude with a summary of microstructural effects on fracture which will emphasize the degree to which they can be

interrelated.

## 2.a. Blunting Studies

While smooth blunting is ordinarily assumed in modeling fracture initiation at initially sharp defects, other blunting geometries such as blunting to two and three corners as shown in Figure 1 were suggested by McClintock [18]. McMeeking [19,20] considered a void of initial radius $R_o$ positioned a distance $X_o$ ahead of an initially sharp crack tip and calculated the void size as a function of $\delta/X_o$. He found, as shown in Figure 2, that while the rates of void growth were initially higher for blunting to two and three corners (or vertices) than for smooth blunting void growth stopped at some point for the case of blunting to vertices while it continued almost linearly in $\delta/X_o$ for smooth blunting. On the basis of these results McMeeking [19,20] suggested that blunting to vertices could result in enhanced toughness.

Studies of crack tip blunting [21,22] utilized two ultra high strength steels HP9-4-20 and HP9-4-10, whose compositions are given in Table 1. Crack tip blunting was examined for both materials in the as-quenched condition and after tempering at 565°C for one hour. The mechanical properties of these four microstructures and the inclusion characteristics for each heat are summarized in Table 2. Note that the inclusion spacings and volume fractions are similar for both materials and that for both materials the tempered microstructures had higher toughnesses than the as-quenched microstructures. Crack tip blunting and hole growth ahead of the blunting crack were investigated for the four microstructures as a function of the J integral or equivalently as a function of the crack tip opening displacement. Our observations suggest that initially (at low $\delta$) it is very difficult to identify the blunting as smooth or to vertices. At some $\delta$, however, less than half of $\delta_{IC}$, blunting behavior for each of the microstructures becomes well defined. The as-quenched specimens blunt smoothly and the tempered specimens blunt to vertices as shown in Figure 3. Furthermore, when compared at the same value of J, the maximum sizes of voids near the blunting crack tips are three to four times smaller for the microstructures which blunt to vertices than for the microstructures which blunt smoothly. (Table 3)

Our conclusion is that blunting to vertices is, under certain circumstances, associated with enhanced toughness. First, for HP9-4-20 tempering at 565°C results in a large increase in the fracture initiation toughness with $\delta_{IC}$ increasing to 93μm compared to 15.5μm for the as-quenched microstructure. This increase in toughness is observed at essentially constant flow stress, a modest increase in the effective plane strain ductility and a decrease in the work hardening exponent (n) from 0.18 to 0.05. Similar behavior was observed for HP9-4-10; tempering increased $\delta_{IC}$ from 43.5μm in the as-quenched

condition to 156μm. This was concomitant with a small increase in the effective plane strain ductility (0.52 to 0.60) and a decrease in n from 0.16 to 0.06. Perhaps the best comparison is between the as-quenched HP9-4-10 and the tempered HP9-4-20. $\delta_{IC}$ for as-quenched HP9-4-10 is 43.5μm compared to 93μm for the tempered HP9-4-20 steel even though the as-quenched HP9-4-10 has a much higher effective plane strain ductility and a higher work hardening exponent. Thus, given that both materials have similar inclusion volume fractions and spacings, the results suggest that if two materials contain the same distribution of inclusions and have the same levels of constrained ductility and one of the microstructures blunts smoothly and the other blunts to vertices, then the microstructure which blunts to vertices will have a considerably higher fracture initiation toughness; data which support this conclusion are presented in a plot of $\delta_{IC}$ versus $X_o\bar{\varepsilon}_f^{ps}$ in Figure 4.

While the notion of blunting to vertices seems to have been accepted for some time, there are apparently no conclusive reports in the literature of blunting to vertices which is microstructurally driven. Knott [23] reports the formation of multiple vertices at blunt crack tips (machined notches in Charpy impact specimens) and McClintock [18] reports several similar examples in the literature. The only example in the literature of blunting to vertices from an initially sharp crack is the blunting of HY80 steel to three corners [24]; this blunting behavior was observed in a single edge-notched tension specimen (SENT) but not in a compact tension specimen and was attributed to lack of constraint associated with SENT specimens. However, it is suggested that the zig-zag fracture observed by Van Den Avyle [25] is associated with blunting to vertices; because Van Den Avyle sectioned his specimens well past crack initiation the blunting behavior cannot be deduced from his micrographs. However, our observations indicate that zig-zag fracture may be observed when blunting to vertices occurs.

Why blunting to vertices is observed in some microstructures but not others is not clear. The study described above, of blunting behavior for HP9-4-20 and HP9-4-10 steels, suggests blunting to vertices is associated with low strain hardening and possibly a tendency for strain localization. It may be also, as suggested by Van Den Avyle [25] in his discussion of zig-zag fracture, that the inclusion spacing is important with larger inclusion spacings favoring blunting to vertices; if inclusion spacing is critical then it may be possible to induce blunting to vertices in the as-quenched microstructures discussed here by increasing the inclusion spacing. An extension of Van Den Avyle's suggestion would be that increasing the resistance to void nucleation at the inclusion could possibly induce blunting to verticies. Finally, given, for a fixed grain size and inclusion type and spacing, that smooth blunting is associated with as-quenched

microstructures characterized by high n and blunting to vertices is associated with heavily tempered microstructures characterized by low n and that for most steels n decreases with increasing tempering temperature it is anticipated that the extent of blunting to vertices will increase as the tempering temperature is increased. Specifically, it is suggested that if a blunted crack tip is sectioned 10 times (for example) then as the tempering temperature is increased the fraction of the ten cross sections which exhibit blunting to vertices will increase with increasing tempering or aging temperature.

## 2.b Control of Inclusion Spacing and the Influence of Inclusion Spacing on Toughness

Some experimental work, the most famous being that of Birkle et al. [8] suggest that as long as the microstructure is otherwise a constant, then the crack tip opening at fracture ($\delta_{IC}$) will scale with the inclusion spacing. The Rice and Johnson model [9] predicts that $\delta_{IC} = X_o F(f)$ where $X_o$ is the inclusion spacing and F(f) is a function which increases slowly with decreasing particle volume fraction, f. While the Rice and Johnson [9] model cannot be used to predict absolute toughness values because it does not include any microstructural parameters other than inclusion spacing it does suggest that if the microstructure remains otherwise constant and if the inclusions can be regarded as pre-existing voids then $\delta_{IC}$ will scale as $X_o$.

In this work particle spacing has been changed by varing inclusion type. To obtain small spacings the sulfur is gettered as manganese sulfides. To obtain larger spacings the sulfur has been gettered as $La_2O_2S$. While manganese sulfides are formed during solidification or possibly precipitated from the solid state during hot working, the $La_2O_2S$ inclusions are apparently formed in the liquid steel [4,5]. The $La_2O_2S$ particles tend to be larger and hence more widely spaced than the manganese sulfide particles because if the lanthanum additions are sufficiently small, changing inclusion type does not change the inclusion fraction. It took about a year to establish a melt practice to successfully use the lanthanum additions. The primary difficulty was that lanthanum forms stable oxides; if too much lanthanum was added then lanthanum reduced the crucible and a large volume fraction of lanthanum oxide was introduced into the material. As long as the steel is carbon deoxidized prior to the late addition of small amounts of lanthanum (0.02 wt%) the inclusions are present at a low volume fraction and at a spacing of 7μm or greater.

The chemistries of three heats of AF1410 steel and of two heats of HY180 steel are given in Table 4. Their inclusion characteristics of the five heats are given in Table 5 and their mechanical properties

after aging at 510°C are summarized in Table 6. As shown in Tables 5 and 6 and Figure 5 increasing the particle spacing results in a substantial improvement in toughness.

What is more interesting is, as shown in Figure 5, that for AF1410 aged at 510°C or 425°C $\delta_{IC}$ does not increase linearly with increasing $X_o$ at constant inclusion volume fraction. While $\delta_{IC}$ does initially increase with $X_o$, the rate of increase decreases with increasing $X_o$. In fact the data in Figure 5 suggest that as $X_o$ increases at constant particle volume fraction $\delta_{IC}$ will approach some limiting value $\bar{\delta}_{IC}$. From the standpoint of improving toughness the results mean that at a constant inclusion volume fraction no improvements in toughness can be realized by increasing the particle spacing beyond some point.

The data shown in Figure 5 and listed in Table 5 and 6 suggest that as $X_o$ and $R_o$ simultaneously become large at some fixed inclusion volume fraction then $\delta_{IC}$ tends to a limiting value denoted $\bar{\delta}_{IC}$. This behavior can be summarized by an equation of the form:

$$\delta_{IC} = \bar{\delta}_{IC} \left( 1 - \exp(-x_o\beta/\bar{\delta}_{IC}) \right) \qquad (1)$$

so that as $X_o$ becomes small, $\delta_{IC} = X_o\beta$ and as $X_o$ becomes large $\delta_{IC}$ approaches $\bar{\delta}_{IC}$. Values of $\beta$ and $\bar{\delta}_{IC}$ for AF1410 and HY180 aged at 510°C are given in Table 7. Moreover, that $\delta_{IC}$ tends to a constant value, $\bar{\delta}_{IC}$, as $X_o$ is increased at constant f does not imply the inclusions no longer influence toughness. The toughness in the absence of inclusions is designated $\delta'_{IC}$ and is in general larger than $\bar{\delta}_{IC}$. Our work with inclusions strongly bonded to the matrix [14] suggests that $\delta'_{IC}$ for HY180 aged at 510°C is at least 890μm (and probably considerably higher) which compares to $\bar{\delta}_{IC}$ = 380μm at f = .00018 for HY180 steel tempered at 510°C Thus it is anticipated $\bar{\delta}_{IC}$ and probably $\beta$ will be influenced by inclusion volume fraction as well as fine scale microstruction.

To obtain expressions for $\bar{\delta}_{IC}$ and $\beta$ as a function of inclusion volume fraction the following procedure has been adopted [13]. Suppose we increase the particle spacing at constant particle size and compare that behavior to that as the particle spacing is increased at some constant inclusion volume fraction. It is expected the dependence of $\delta_{IC}$ on $X_o$ at constant particle size will be something like the curve in Figure 6. At sufficiently small $X_o$ $\delta_{IC}$ should be linear in $X_o$ and will be lower than that obtained at constant f at the same particle spacing, the constant f and constant $R_o$ curves intersect at some particle spacing, and as $X_o$ increases at constant particle size $\delta_{IC}$ will approach $\delta'_{IC}$ because the volume fraction will go to zero as spacing is increased at constant particle size. Furthermore because the curves of $\delta_{IC}$

versus $X_o$ for different constant particle sizes will cross the constant volume fraction $\delta_{IC}$ *vs* $X_o$ curve at different $X_o$ (the $X_o$ for cross over increases with particle size) the shape of each curve of $\delta_{IC}$ *vs* $X_o$ for a constant particle size will depend on the particle size. A simple formula relating $\delta_{IC}$ *vs* $X_o$ for constant particle size which satisfies these requirements is:

$$\delta_{IC} = \delta'_{IC}\left(1 - \exp(-x_o h(R_o,f)/\delta'_{IC})\right) \tag{2}$$

If it is assumed that $h(R_o,f) = g(R_o)f^{-\alpha}$ then an expression for $g(R_o)$ can be obtained by requiring equations 1 and 2 to provide the same results at some fixed volume fraction for which $\beta$ and $\overline{\delta}_{IC}$ are known. The justification for making the assumption $h(R_o,f) = g(R_o)\, f^{-\alpha}$ is the following. Rice and Johnson predict that for a fixed fine scale microstructure $\delta_{IC} = X_o F(f)$ where $F(f)$ is a function which increases slowly as the inclusion volume fraction $f$ is decreased. The calculations of Rice and Johnson suggest $F(f) \approx f^{-\alpha}$ where $1/6 < \alpha < 1/9$. Furthermore, the solution for $g(R_o)$ obtained making this assumption yields, in the limit of small particle spacing, $\delta_{IC} = X_o C f^{-\alpha}$ where C is a function only of the microstructure; thus the assumption yields a solution consistent with Rice and Johnson in the limit of $X_o$ small. Once $g(R_o)$ is obtained it can be shown that if $\beta$ and $\overline{\delta}_{IC}$ are known at one volume fraction $f = f_{ref}$ and if $\delta'_{IC}$ is known, then $\beta$ and $\overline{\delta}_{IC}$ at any volume fraction can be obtained:

$$\beta(f) = \beta(f_{ref}) f^{\alpha}_{ref}/f^{\alpha} \tag{3}$$

$$\overline{\delta}_{IC}(f) = \delta'_{IC}\left(1 - (1 - \overline{\delta}_{IC}(f_{ref})/\delta'_{IC})^{(f_{ref}/f)^{1/3+\alpha}}\right) \tag{4}$$

Using $\delta_{IC}$ measured for inclusions strongly bonded to the matrix as a lower bound for $\delta'_{IC}$ (see Table 7) curves of $\delta_{IC}$ as a function of $X_o$ for a fixed volume fraction can be obtained. Such curves are shown in Figure 7 for HY180 steel aged at 510°C assuming $\alpha = 1/7$. The results suggest that $\delta'_{IC}$ can be approached by reducing the inclusion volume fraction to low levels. Assuming $\alpha = 1/7$, the volume fractions required are low, but inspection [26] of the data of Birkle et al. [8] suggests the dependence of toughness on inclusion volume fraction is stronger than predicted by Rice and Johnson and that $\alpha$ is closer to a third than the $1/6 < \alpha < 1/9$ suggested by their calculations.

The data in Figure 5 suggests that at a fixed inclusion volume fraction $\delta_{IC}$ is linear in $X_o$ only when $X_o$ is small and that $\delta_{IC}$ approaches some constant value, $\overline{\delta}_{IC}$, as $X_o$ and $R_o$ simultaneously increase. The approach taken to describing this behavior leads to a function, $g(R_o)$, which is a function only of the microstructure and of the average inclusion size $R_o$ [13]. In the limit of small $R_o$, $g(R_o)$ approaches a

value which is a function only of the fine scale microstructure; as $R_o$ increases $g(R_o)$ decreases. While $g(R_o)$, under the assumptions made, is sufficient to rationalize the observed behavior it represents a formal but not a physical explanation of this behavior. Two interpretations of this behavior are possible [13]. The first is that $\delta_{IC}$ becomes explicitly a function of particle size and particle size does not influence toughness just through the ratio $X_o/R_o$ which defines $f(X_o/R_o = .89f^{-1/3})$. That is, a limiting value, $\overline{\delta}_{IC}$, is reached at constant f because of a competition between increasing $X_o$ (beneficial to toughness) and increasing $R_o$ (detrimental to toughness).

An alternative explanation for the observed dependence of $\delta_{IC}$ on $X_o$ at constant particle volume fraction is that particle spacing has no influence on toughness at constant f once $X_o$ exceeds some critical distance. For spacings greater than this critical distance inclusions influence toughness primarily through the volume fraction. A case for an explicit particle size dependence is hard to make; the most obvious possible explanation is that increasing the particle size makes void nucleation easier; however, conditions for void nucleation at the closely spaced particles (MnS) and the larger more widely spaced particles ($La_2O_2S$) appear to be the same, at least for HY180 tempered at 510°C, as shown in Figure 8. It is suggested instead that particle spacing significantly influences toughness only when the particle spacing is on the order of or less than the effective grain size, in these materials the martensite packet size. Strain localization appears to be an important aspect of fracture in these materials. Apparently strain localization can be achieved much more readily in single crystals than in equivalent bodies containing many grains [27]. So it may be that if the inclusions are separated by several grains strain localization driven by the strain concentrations around the growing voids will be more difficult to achieve than if the inclusion spacing is on the order of or less than the grain size. If this is the case it would be appropriate to write $g(R_o) = g(X_o,f)$. When this is done a characteristic distance emerges which is on the order of the prior austenite grain size or 3 to 4 times the packet size [13].

## 2.c. Influence of Undissolved Carbides/Nitrides

The conventional picture of how the carbides and nitrides inherited from the austenitizing temperature might enter the fracture process is drawn from the observations of Cox and Low (28). As shown in Figure 9 the voids nucleated at the inclusions grow until they impinge or until they coalesce via the formation of a void sheet where the voids in the void sheet are nucleated at the undissolved carbides. Certainly we expect the effects of such particles to be detrimental to the toughness and we will present some results to illustrate their effects.

The two heats to be discussed are two heats of HP9-4-20 steel designated heats 1 and heat 2 and their properties are compared in the as-quenched condition [29]. The chemistries of the two heats are in Table 8 and their inclusion characteristics and mechanical properties are compared in Tables 9, 10, and 11. Note that after austenitizing at 840°C, $\delta_{IC}$ for heat 2 is 15μm compared to 10μm for heat 1; this is despite the inclusions in heat 1 having a larger spacing ($X_o$ = 3.7μm) than the inclusions in heat 2 ($X_o$ = 2.5μm). The sulfides are MnS for both materials and the spacings are sufficiently small that $\delta_{IC}$ is still reasonably linear in $X_o$. The only microstructural differences which can explain this apparent contradiction are differences in the undissolved carbides and/or nitrides. The two heats have the same prior austenite grain size and the same retained austenite content.

Extraction replicas of polished cross sections were used to determine the types, sizes and volume fractions of undissolved carbides and nitrides present in the materials. In addition, extraction replicas were made of fracture surfaces to determine which of these particles were active in the fracture process.

The results from extraction replicas from polished cross sections can be summarized as follows. In heat 1 there were two types of particles. Most of the particles were cuboidal and had a fcc NaCl type structure with a lattice parameter of 4.2 Å, similar to TiC, VC, and TiN and carbonitrides of this type. These particles contain primarily Ti and V with smaller amounts of Al and Mo. As they could not be dissolved by using high austenitizing temperatures it was concluded they were complex carbonitrides and not simply carbides, this is consistent with the high nitrogen content of this heat. A second type of particle was also observed. They were rod like, considerably larger and had an hcp structure corresponding to $Mo_2C$. They contained primarily Mo with smaller and variable amounts of Cr, Ti, and V. It was concluded they were $M_2C$ particles of complex composition. Based on qualitative chemical analysis of many particles and on the particle shapes these particles constituted only 8% of the total number of particles.

For heat 2 there were also two types of particles. There were large, rod like particles which again could be indexed as $M_2C$ with compositions similar to those observed in heat 1 except there were smaller levels of Ti. The second type of particle was again of the M(C,N) type. These particles much smaller than the $M_2C$ particles and contained primarily V. As they could be readily dssolved at 1050°C it was concluded they were VC and not nitrides or carbo-nitrides. Because of the very small size of these VC particles the $M_2C$ particles constituted less than 1% of the total particle number in heat 2.

The average size of these particles in the bulk materials are given in Table 12. Note that the

particles in heat 1 are much larger than those in heat 2, with the average particle diameters being about 500Å for heat 1 and about 134 Å for heat 2. These differences reflect primarily the differences in sizes of the M(C,N) particles in the two heats due to the small percentages of $M_2C$ particles. The maximum dimensions of the $M_2C$ particles were about 800Å and 600Å in heat 1 and heat 2 respectively.

Extraction replicas of fracture surfaces yielded the following information. For heat 1 both the $M_2C$ and the M(C,N) particles nucleated voids. However, 30% of the particles which nucleated voids were $M_2C$ compared to 8% in the bulk. For heat 2 almost all of the secondary voids were nucleated by the $M_2C$ particles and the VC particles were rarely observed to nucleate secondary voids. These results suggest the higher toughness of heat 2 was due to differences in the M(C,N) type particles.

In interpreting the effects of undissolved carbides and nitrides it would seem reasonable to conclude that the fine VC particles in heat 2 which rarely nucleate secondary voids are to be preferred to the larger Ti(C,N) particles in heat 1 which are very active in the fracture process. Second, it would appear $M_2C$ particles which are larger than the M(C,N) type particles in either heat are much more active in the fracture process than would be suggested by their numbers. Therefore the results suggest fine VC carbides are the least detrimental to toughness, the $M_2C$ carbides are the most detrimental and the large Ti(C,N) particles in heat 1 are intermediate in their influence on toughness, although they appear to be considerably worse than the fine VC particles in heat 2.

The above work suggests that one can identify the types, chemistries and sizes of the fine undissolved carbides and nitrides inherited from the austenitizing treatment. Furthermore the volume fractions can be determined (at least up to a factor of 2) by using extraction replicas from lightly and heavily etched polished cross sections according to the methods outlined by Stumpf and Sellars [30]. One can also determine which of these particles are active in the fracture process by examining extraction replicas of fracture surfaces. Quantifying the influence of these particles is more difficult. It would be desirable to assess their influence on fracture toughness by measuring a property which is related to toughness but which is not influenced by inclusion volume fraction or spacing. As noted earlier, for a fixed blunting behavior and small inclusion spacings, $\delta_{IC}$ appears to scale with the product $X_o\bar{\varepsilon}_f^{ps}$ where $X_o$ is the particle spacing and $\bar{\varepsilon}_f^{ps}$ is the effective plane strain tensile ductility. Speich and Spitzig [31] have shown that at high strength levels $\bar{\varepsilon}_f^{ps}$ is not influenced by inclusion volume fraction, nor does it appear to be influenced by inclusion spacing [12]. However, $\bar{\varepsilon}_f^{ps}$ does appear sensitive to changes in the distributions of undissolved carbides. For the two heats of HP9-4-20 considered here, $\bar{\varepsilon}_f^{ps}$ was 0.15 for

heat 1 and 0.25 for heat 2. It is suggested that the effective plane strain tensile ductility provides a useful manner of assessing the influence of undissolved carbides and/or nitrides on fracture toughness.

## 2.d. Influence of Grain Size

When these two heats of HP9-4-20 steel are austenitized at 1050°C $\delta_{IC}$ for heat 1 increases to 23μm but $\delta_{IC}$ for heat 2 does not change (Table II). The toughness of heat 1 increases because of an increase in the inclusion spacing attributed to the dissolution of the finer MnS particles and because of the dissolution of the $M_2C$ particles. On austenitizing at 1050°C the inclusion spacing in heat 1 increases slightly; in addition there is dissolution of the $M_2C$ particles and almost all of the VC particles. The toughness of heat 2 should have increased.

The changes in inclusion characteristics, mechanical properties and undissolved carbides for the two heats after austenitizing at 840°C and 1050°C are summarized in Tables 9-12. On austenitizing at 840°C the two heats have the same grain size (12μm) but on austenitizing at 1050°C the grain size of heat 1 increases to 26μm but that of heat 2 increases to 66μm. It is believed the unexpectedly low toughness of heat 2 after austenitizing at 1050°C is due to this large grain size. The effect of grain size on toughness is probably complex and is possibly related to the inclusion spacing; if the grain size increases without an increase in inclusion spacing it is likely that the inclusions become more detrimental to toughness for reasons discussed earlier.

Therefore, dissolving the fine carbides may reduce their potential direct influence on fracture toughness, but the dissolution of these particles can lead to grain growth which may have an indirect and adverse effect on toughness, the magnitude of which will possibly be related to the ratio of the grain size to inclusion spacing.

## 2.e. Studies of Void Nucleation and Growth

Since the approach to changing inclusion spacing has been to change particle type, i.e. replacing MnS by $La_2O_2S$ particles, one may suspect that changes in toughness which are ascribed to changes in particle spacing may be due instead to differences in void nucleation characteristics. Therefore a program was begun to examine void nucleation for MnS and $La_2O_2S$ inclusions as a function of microstructure and strength level. The materials selected were two heats of HY180 steel, one heat containing MnS inclusion and one heat containing $La_2O_2S$ inclusions. Similar heats of the higher strength steel AF1410 were also prepared. As shown in Table 4 the composition of AF1410 is identical to that of HY180 except for a higher carbon content (0.16 wt% compared to 0.10 wt%) and a higher cobalt content

(14 wt% compared to 8 wt%). Void nucleation is being studied for the as-quenched microstructures (high n) and the tempered at 510°C microstructures (low n). The inclusion characteristics of the four heats being used are shown in Table 5 (heat 1 and heat 2 for AF1410).

The approach has been to cross section fractured smooth axisymmetric tensile specimens to the mid-plane and then determine the total volume fraction of voids and particles as a function of strain. This volume fraction normalized by the initial inclusion volume fraction is then plotted as a function of strain. Initially this normalized volume fraction will be 1 but will increase once voids have nucleated. Using this data and studies of necking geometry in various specimens it is planned to determine the critical interfacial stress required to nucleate voids at the different inclusions [15,16,33].

While the results are still incomplete they suggest that MnS sulfides and $La_2O_2S$ have similar void nucleation characteristics. As shown in Figure 8 the data for MnS and $La_2O_2S$ in HY180 steel aged for 5 hours at 510°C are almost the same. It appears that void nucleation and growth is influenced by microstructure as shown by the results for MnS in HY180 steel in the as-quenched and tempered conditions in Figure 10. In addition void nucleation occurs at lower strains at higher strength levels as shown by the results in Figure 11 for MnS in HY180 steel ($\sigma_{y,s}$ = 1200 MPa) and in AF1410 steel ($\sigma_{y,s}$ = 1530 MPa) aged at 510°C.

In addition to this work we have investigated the effect of replacing MnS or $La_2O_2S$ inclusions in HY180 steel by particles believed to be $Ti_2CS$ inclusions. The chemistries of the three heats of HY180 steel and the sulfides presented in each heat are given in Table 13. The properties of these heats are compared in Table 14 and the inclusion characteristics of the three heats are summarized in Table 15. The substantial improvements in toughness which can be achieved by utilizing the $Ti_2CS$ sulfides has already been noted [14]. This improvement in toughness appears to be related to strong bonding between the matrix and the $Ti_2CS$ particles. As shown in Figure 12 void growth is appreciable in the heat containing MnS at a strain of about 0.7 but a similar extent of void growth requires a strain of 1.3 for the heat containing $Ti_2CS$ particles. Wavelength dispersive spectrometry suggests these particles contain Ti, C and S. The only particles which have this chemistry and which have been identified in steels are $Ti_2CS$ [34-36], however work is in progress to unequivocally identify these particles.

The enhanced toughness of the heat containing the$Ti_2CS$ inclusions is attributed to the improved resistance to void nucleation of these particles. This conclusion appears justified because the inclusion

volume fractions were almost the same (Table 15) and the titanium additions (0.02 wt%) should result not only in titanium carbosulfides but in the formation of TiC particles which should degrade toughness. While the quantification of the undissolved carbides in the two heats is not complete, extraction replicas of as-quenched polished cross sections indicate that the undissolved carbides and/or nitrides in the two heats are of about the same size but they are, based on the number per unit area in TEM micrographs of the extraction replicas, about 10 times more numerous in the heat containing the titanium carbosulfides.

It is suggested that utilizing $Ti_2CS$ to getter sulfur offers the potential for improving the upper shelf toughness for many steels; certainly this is indicated by the data in Fig. 13. The Ti additions used to date have been 0.02 wt%. If the sulfur level is 0.0015 wt% then only .0044 wt% titanium is required to getter all of the sulfur as $Ti_2CS$; the remaining Ti would be available to form TiC or other particles. The detrimental effects of these particles will increase as the strength level increases even if the TiC volume fraction and size stay fixed [17]. Moreover, if the carbon content increases the TiC volume fraction and size should increase. Therefore in using this approach it would appear critical to use just enough titanium to form the $Ti_2CS$.

At the present time we do not know why the particles believed to be $Ti_2CS$ are more resistant to void nucleation. In all of the steels examined, except for those modified by lanthanum additions, void nucleation is by particle/matrix decohesion. For the case of void nucleation by decohesion of the particle-matrix interface it has been suggested that decohesion will occur at some critical interfacial stress [32,33]. Argon and coworkers [15,16,33] have suggested the stress normal to the matrix-particle interface ($\sigma_I$) can be taken to be $\sigma_I = \sigma_f + \sigma_H$, where $\sigma_f$ is the flow stress of the material and $\sigma_H$ is the hydrostatic component of the stress. According to the critical stress theory, void nucleation will occur when $\sigma_I$ reaches some critical value. This critical stress can be deduced from the results of the experiments outlined above. Others, however, have suggested that local plastic strain, and not just $\sigma_f$ and $\sigma_H$ contribute to the interfacial stress [32,37-39]. Moreover, such an important issue as the influence of particle size on void nucleation remains unanswered with some arguing that small particle size will increase resistance to void nucleation [40], others arguing the opposite [37] and some arguing no role of particle size [33]. It is suggested that void nucleation is related critically to the nature of the chemical bonding at the interface and possibly to the structure of the interface as well. However, it seems clear that understanding why the $Ti_2CS$ particles are more resistant to void nucleation will require a better understanding of the process of void nucleation.

## 2.f. Microstructure and Fracture

The foregoing suggests that the inclusions, undissolved carbides and/or carbo-nitrides can directly influence the fracture initiation toughness of ultra high strength steels and that blunting behavior is an important consideration as it appears to reflect fundamental changes in the micromechanisms of the fracture process. In discussing the fracture of ultra high strength steels the following microstructural approach is useful, if somewhat artificial, as it illustrates both the complexity of the fracture process and the degree to which effects on toughness of various microstructural features can be interrelated. In this approach the microstructure is divided into three categories: primary particles, secondary particles inherited from the austenitizing treatment and the fine scale microstructure.

The primary particles in steels are the inclusions. They are normally regarded as the particles at which voids are first nucleated. Primary particle spacing, volume fraction and void nucleation characteristics can all influence fracture toughness. Their influence is direct, through the nucleation and growth of voids, although the work of Van Den Avyle [25] suggests they may indirectly influence fracture if blunting behavior can be altered by primary particle spacing.

In addition to the primary particles there are secondary particles. Secondary particles can be fine particles inherited from the austenitizing treatment or particles precipitated during tempering. It is expected that void nucleation will be much more difficult at the secondary particles and they will be activated much later (or possibly not at all) in the fracture process than are the primary particles. Cox and Low [28] have illustrated how the secondary particles might influence the fracture process. As shown in Figure 9, the voids nucleated at the primary particles can grow either until they impinge or until they coalesce via the formation of a void sheet where the voids in the void sheet are nucleated at the secondary particles. However, as noted earlier, it may be that this picture is substantially an over simplification of the role of secondary particles particularly for the case of blunting to vertices where shear fracture associated with the zig-zag fracture path appears to be more important than for the case of smooth blunting.

The secondary particles inherited from the austenitizing temperature include undissolved carbides, nitrides and complex carbo-nitrides. They typically are present in such low volume fractions that they do not contribute to the strength of the steel. They can directly influence the fracture process if they actually nucleate voids and they can indirectly influence the fracture process by influencing the prior austenite grain size.

All microstructural features other than the primary particles and the secondary particles inherited from the austenitizing temperature are regarded as the fine scale microstructure. The fine scale microstructure can directly influence the fracture process if particles precipitated on aging actually nucleate voids. The particles precipitated on aging can indirectly influence the fracture process by their role in determining the flow properties of the material. The flow properties can influence void nucleation and growth and apparently the nature of the crack tip blunting as well. Other microstructural features may indirectly influence the fracture process. These include the prior austenite grain and martensite packet sizes, the amount, morphology and mechanical stability of the austenite and the dislocation structure. As noted earlier, the effective grain size, probably the packet size may determine the range of primary particle spacing over which primary particle spacing influences toughness [13]. In addition, since the undissolved carbides and/or nitrides inherited from the austenitizing treatment can influence grain size and large grain size appears detrimental to toughness [29], at least at small primary particle spacings, minimizing the direct influence on toughness of undissolved carbides by using high austenitizing temperatures may not be as effective in improving toughness as anticipated if there is a large increase in grain size.

## 3. Summary of Accomplishments

I feel this research program has been effective in terms of both quality and quantity of effort. Here the four major technical achievements are summarized and degrees granted, papers published or submitted and industrial involvement enumerated. Currently one second year Ph.D. student is completely supported by this contract.

## 3.a. Technical Highlights

The following are the four most important results to date:

1. Able to control inclusion spacing in a systematic manner applicable to many alloys produced by VIM/VAR melting. To obtain large inclusion spacings lanthanum is used to getter the sulfur as $La_2O_2S$ particles formed in the liquid steel. If the lanthanum additions are sufficiently small the inclusion volume fraction is small. The increased particle spacing results in significant improvements in toughness.

2. Shown that at constant particle volume fraction the crack tip opening displacement at fracture ($\delta_{IC}$) initially increases with particle spacing, but that the rate of increase decreases with increasing particle spacing. As the particle spacing becomes large at constant particle volume fraction, $\delta_{IC}$ appears to approach a constant value, so that when the particle

spacing exceeds some critical spacing, $\delta_{IC}$ becomes independent of $X_0$.

3. Made the first observations of blunting to vertices at sharp cracks which is microstructurally driven. Observations made in the context of controlled inclusion volume fraction and spacing and systematic microstructural variations which permit the influence of blunting behavior on fracture toughness to be assessed.

4. Found that if $La_2O_2S$ or MnS inclusions are replaced by particles rich in titanium, sulfur and carbon and believed to be $Ti_2CS$ then tremendous improvements in toughness can be obtained. This effect is attributed to resistance to void nucleation at these particles.

## 3.b. Degrees Granted:

Mr. J. W. Bray
Degree: M.E.
Title: Microstructure-Fracture Toughness Relationships in Particle Containing Alloys

Dr. K. J. Handerhan
Degree: Ph.D.
Title: The Effects of Microstructure on the Crack Initiation Toughness of High Strength Secondary Hardening Steels

## 3.c. Papers


1. W.M. Garrison, Jr. and N. R. Moody, "Ductile Fracture", an invited review article on ductile fracture for The Journal of Physics and Chemistry of Solids, 1987, Vol. 48, 1035-1074.

2. W.M. Garrison, Jr. and K. Handerhan, "Fracture Toughness: Particle Dispersion Correlations", in Proceedings of 34th Sagamore Army Materials Research Conference on Innovations in Ultra High Strength Steels, held September 1987 at Lake George. Invited paper.

3. K.J. Handerhan and W.M. Garrison, Jr., "Effects of Rare Earth Additions on the Mechanical Properties of the Secondary Hardening Steel AF1410", Scripta Met., 1988, Vol. 22, 409-412.

4. K.J. Handerhan and W.M. Garrison, Jr., "Observations on the Upper Shelf Crack Tip Blunting Behavior of Ultra High Strength Steels", Scripta Met., 1988, Vol 22, 607-610

5. J.L. Maloney and W.M. Garrison, Jr., "A Study of Void Nucleation and Growth at MnS and $Ti_2CS$ Inclusions in HY180 Steel", Scripta Metall., 1989, Vol 23, 2097-2100

6. K.J. Handerhan and W.M. Garrison, Jr., "The Effect of Austenitizing Temperature on the Fracture Initiation Toughness of As-Quenched HP9-4-20 Steel" Metall. Trans. A, 1988, Vol 19A, pp 2989-3003

7. K.J. Handerhan and W.M. Garrison, Jr., "A Comparison of the Fracture Behavior of Two Heats of the Secondary Hardening Steel AF1410" Metall. Trans. A, 1989, Vol 20A, pp 105-123

8. K.J. Handerhan and W.M. Garrison, Jr., "A Study of Crack Tip Blunting Behavior and the Influence of Blunting Behavior on the Fracture Toughness of Ultra High Strength Steels" submitted to Acta Metall.

9. K.J. Handerhan and W.M. Garrison, Jr., "A Comparison of the Influence of Austenitizing Temperature on the As-Quenched Fracture Toughness of Two Heats of HP9-4-20 Steel", submitted to Metall. Trans. A.

10. J.W. Bray, J.L. Maloney, K.S. Raghavan and W.M. Garrison, Jr., "A Comparison of the Fracture Behavior of Two Commercially Produced Heats of HY180 Steel Differing in Inclusion Type", submitted to Metall. Trans. A.

11. K.S. Raghavan, W.M. Garrison, Jr. and J.L. Maloney, "A Comparison of Void Nucleation at Inclusions in Two Heats of AF1410 Steel Containing either Manganese or Chromium Sulfides", submitted to Metall. Trans. A.

12. K.J. Handerhan and W.M. Garrison, Jr., "Surface Roughness and the Fracture Initiation Toughness of Ultra High Strength Steels", submitted to Metall. Trans A.

## 3.d. Industrial Involvement

1. Latrobe Steel:

   Support and contribute to research expenses of J.L. Maloney whose Ph.D. thesis will be finished in the Fall of 1989.

2. Ellwood City Forge

   Supported and contributed to research expenses of K.J. Handerhan whose Ph.D. thesis was completed in Fall of 1987.

3. Teledyne-Allvac

   Contributed ten 100 lb VIM/VAR heats as well as commercially produced material.

4. Teledyne-Vasco

   Carried out all upsetting and cross forging of experimental heats.

5. Cytemp:

   Contributed over 1000 lbs of AF1410 modified by lanthanum additions.

## 3.e. Patent Application

1. W.M. Garrison, Jr. and J.L. Maloney; application made for patent "Control of Inclusion Types to Improve the Fracture Toughness of Ultra High Strength Steels".

## References


1. G.R. Speich, D.S. Dabkowski and L.F. Porter, Metall. Trans., 1973, vol. 4, 303.
2. G.D. Little and P.M. Machmeier, The Development of a Weldable High Strength Steel, Technical Report AFML-TR-75-148. Air Force Materials Laboratory, Wright Patterson, Ohio.
3. W.M. Garrison, Jr. and N.R. Moody, [Metall. Trans. A], 1987, vol. 18A, 1257.
4. L. Luyckx, J.R. Bell, A. McLean and M. Korchynsky, Metall. Trans., 1970, vol. 1, 3341.
5. P.E. Waudby, "Rare Earth Additions to Steel", Int. Metals Review, 1978, No. 2, 74.
6. D.C. Hilty and J.W. Farrell, "Modifications of Inclusions by Calcium", Conference Proceedings, Inclusions and Their Effects on Steel Properties, University of Leeds, September 1974, British Steel Corporation.
7. W.A. Spitzig, Trans. ASM, 1968, vol. 61, 344.
8. A.J. Birkle, R.P. Wei and G.E. Pellissier, Trans. ASM, 1966, vol. 59, 981.
9. J.R. Rice and M.A. Johnson, "The Role of Large Crack Tip Geometry Changes in Plane Strain Fracture", Inelastic Behavior of Solids, M.F. Kanninen, W.G. Adler, A.R. Rosenfield and R.I. Jaffee, eds., McGraw-Hill, New York, 1970, 641.
10. W.M. Garrison, Jr., Metall. Trans A, 1986, vol. 17A, 669.
11. K.H. Handerhan and W.M. Garrison, Jr., Metall. Trans. A, 1988, vol. 19A, 2989-3003.
12. K.J. Handerhan and W.M. Garrison, Jr., Metall. Trans. A, 1989, vol. 20, 105-123.
13. W.M. Garrison, K.S. Raghavan and J.L. Maloney, "A Discussion of the Influence of Particle Spacing on Fracture Toughness at Constant Particle Volume Fraction", submitted to Metall. Trans. A
14. J.L. Maloney and W.M. Garrison, Jr., "A Study of Void Nucleation and Growth at MnS and $Ti_2CS$ Inclusions in HY180 Steel", Scripta Metall., 1989, vol. 23, 2097-2100.
15. A.S. Argon, J. Im, and R. Safoglu, Metall. Trans., 1975, 6A, 825.
16. A.S. Argon and J. Im, Metall. Trans., 1975, 6A, 839.
17. J.A. Psioda, "The Effect of Microstructure, Strength on the Fracture Toughness of an 18Ni. 300 Grade Maraging Steel", Ph.D. Thesis, Carnegie Mellon University, 1977.
18. F.A. McClintock, "Plasticity Aspects of Fracture," Fracture: An Advanced Treatise, ed. H. Liebowitz, Academic Press, New York, 1974, Vol. 3, p. 47.
19. R.M. McMeeking, J. Mech. Phys. Solids, 1977, 25, 357.
20. R.M. McMeeking, J. Engng. Mater. Technol. Trans., ASME, 1977, 99, 290.
21. K.J. Handerhan and W.M. Garrison, Jr., Scripta Met., 1988, vol. 22, 607-610.
22. K.J. Handerhan and W.M. Garrison, Jr., "A Study of Crack Tip Blunting and the Influence of Blunting Behavior on the Fracture Toughness of Ultra High Strength Steels", submitted to Acta Metall.
23. J.Q. Clayton and J.K. Knott, Metal Sci., 1977, vol. 10, 290.
24. J.W. Hancock and M.J. Cowling, Conference Proceedings: "Micromechanisms of Crack Extension (Mechanics and Physics of Fracture 11)," Cambridge, in Metal Science, 1980, 14, 293.
25. J.A. Van Den Avyle, "Correlation of Fractography, Microstructure and Fracture Toughness Behavior of High Strength Alloys," Ph.D Thesis, M.I.T., 1975.

26. W.M. Garrison, Jr. and K.S. Raghavan, "A Discussion of the Results of Birkle et al. on the Influence of Particle Spacing on Fracture Toughness," submitted to Metall. Trans. A.

27. S.V. Harren, H.E. Deve and R.J. Asaro, Acta Met., 1989, vol. 36, 2435-2480.

28. T.B. Cox and J.R. Low, Metall. Trans., 1974, 5, 1457.

29. K.J. Handerhan and W.M. Garrison, Jr., "A Comparison of the Influence of Austenitizing Temperature on the As-Quenched Fracture Toughness of Two Heats of HP9-Y-20 Steel," submitted to Metall. Trans. A.

30. W.E. Stumpf and C.M. Sellars, Metallography, 1968, vol. 1, 25-34.

31. G.R. Speich and W.A. Spitzig, Metall. Trans., 1982, vol. 13A, 2239.

32. M. Ashby, Phil. Mag., 1966, 14, 1157.

33. A.S. Argon and J. Im, Metall. Trans. A, 1975, vol. 6A, 839.

34. L. Meyer, F. Heisterkamp and D. Lauterborn, in "Processing and Properties of Low Carbon Steel", J.M. Gray, ed., p. 297. The Metallurgical Society of AIME, Warrendale, PA, 1973.

35. T.J. Baker, JISI, 1972, 210, 793.

36. R.D.K. Misra, T.V. Balasubramanian and P. Rama Rao, J. of Mat. Sci. Letters, 1987, 6, 125.

37. S.H. Goods and L.M. Brown, Acta Metall., 1979, 27, 1.

38. J.R. Fisher and J. Gurland, Metal. Sci., 1981, vol. 15, 185.

39. J.R. Fisher and J. Gurland, Metal. Sci., 1981, vol. 15, 193.

40. R.H. Van Stone, T.B. Cox, J.R. Low and J.A. Psioda, Int. Metals Rev., 1985, vol. 30(4), 157.

## 5. Tables and Figures

### Table I

### Chemistries of Heats of HP9-4-20 and HP9-4-10 Steels*

| Alloy | C | Co | Ni | Cr | Mo | V | Mn | P | S | Si | Al | Ti | O | N |
|---|---|---|---|---|---|---|---|---|---|---|---|---|---|---|
| HP9-4-20 | 0.21 | 4.3 | 8.6 | .77 | .94 | .09 | .26 | .005 | .002 | .04 | .009 | .004 | .0013 | .002 |
| HP9-4-10 | 0.10 | 3.9 | 8.9 | .76 | 1.02 | .10 | .31 | .004 | .002 | .01 | .001 | nil | .001 | .0002 |

*Compositions in wt%.

## Table II

## Mechanical Properties and Inclusion Data for Heats of HP9-4-20 and HP9-4-10 Steels

| Alloy | $\sigma_y$ ($MN/m^2$) | $\sigma_u$ ($MN/m^2$) | $\sigma_o$ ($MN/m^2$) | n | $\varepsilon_f$ | $J_{IC}$ (MN/m) | $\delta_{IC}$ (μm) | $\bar{\varepsilon}_f$ | f | $R_0$ (μm) | $X_0$ (μm) |
|---|---|---|---|---|---|---|---|---|---|---|---|
| HP9-4-20 | | | | | | | | | | | |
| A.Q. | 1154 | 1667 | 1411 | .18 | 1.05 | .05 | 16 | .25 | .00022 | .17 | 2.5 |
| 565°C | 1247 | 1379 | 1313 | .05 | 1.25 | .206 | 93 | .37 | | | |
| HP9-4-10 | | | | | | | | | | | |
| A.Q. | 949 | 1269 | 1109 | .16 | 1.21 | .111 | 43 | .52 | .00036 | .19 | 2.4 |
| 565°C | 1056 | 1178 | 1117 | .06 | 1.41 | .264 | 156 | .60 | | | |

$\sigma_y$ is the yield strength; $\sigma_u$ is the ultimate tensile strength, $\sigma_0$ is the flow stress $((\sigma_y + \sigma_u)/2)$; $\varepsilon_f$ is the fracture strain from smooth axisymmetric tensile specimens; $\bar{\varepsilon}_f$ is the effective plane strain tensile ductility. f is the inclusion volume fraction; $R_0$ is the average inclusion radius; $X_0$ is the average nearest neighbor distance in a volume calculated from $X_0 = .89\, R_0 f^{-1/3}$.

## Table III

## Maximum Apparent Void Radius from Sectioned J Specimens

| Microstructure | J @ Unloading (MPa-m) | Maximum Void Radius (μm) |
|---|---|---|
| HP9-4-20 | | |
| A.Q. | 0.032 | 5.3 |
| 565°C | 0.028 | 1.0 |
| HP9-4-10 | | |
| A.Q. | 0.049 | 6.0 |
| 565°C | 0.044 | 2.5 |

# Table IV

## Chemistries of Heats of AF1410 and HY180 Steels

| Material | C | Co | Ni | Cr | Mo | V | Mn | P | S | Si | Al | O | N | La |
|---|---|---|---|---|---|---|---|---|---|---|---|---|---|---|
| AF1410 | | | | | | | | | | | | | | |
| heat 1 | 0.16 | 14 | 9.97 | 2.04 | 1.0 | .001 | .001 | .004 | .001 | .01 | .003 | .001 | .0009 | <.002 |
| heat 2 | 0.16 | 14. | 10.1 | 2.1 | 1.0 | .001 | .03 | .004 | .001 | .03 | .003 | .0009 | .0003 | .012 |
| heat 3 | 0.16 | 13.8 | 10.1 | 1.95 | 0.99 | - | .02 | .003 | .001 | .02 | - | - | - | .008 |
| HY180 | | | | | | | | | | | | | | |
| heat 1 | 0.10 | 7.96 | 9.86 | 1.98 | 1.02 | - | 0.31 | .004 | .002 | .01 | - | .0006 | .0003 | <.002 |
| heat 2 | 0.12 | 8.07 | 9.88 | 1.99 | 1.0 | - | 0.01 | .003 | .001 | .01 | - | .0008 | .0003 | .005 |

## Table V

## Inclusion Characteristics of Heats of AF1410 and HY180 Steels

| Material | type | f | $R_0$ (μm) | $X_0$ (μm) |
|---|---|---|---|---|
| AF1410 | | | | |
| heat 1 | CrS | 0.00034 | 0.18 | 2.3 |
| heat 2 | $La_2O_2S$ | 0.00042 | 0.64 | 7.6 |
| heat 3 | $La_2O_2S$ | 0.00036 | 1.05 | 12.4 |
| HY180 | | | | |
| heat 1 | MnS | 0.00021 | 0.16 | 2.4 |
| heat 2 | $La_2O_2S$ | 0.00015 | 0.44 | 7.5 |

f = volume fraction

$R_0$ = average radius of inclusions

$X_0$ = average nearest neighbor distance in volume ($X_0 = .89\ R_0 f^{-1/3}$)

# Table VI

## Mechanical Properties of Heats of AF1410 and HY180 Steels Aged at 510°C

| Material | Yield Strength (MPa) | UTS (MPa) | $\epsilon_f^{AXS}$ ($ln\,(A_0/A_f)$) | $\bar{\epsilon}_f^{P.S.}$ ($(ln(t_0/t_f))2/\sqrt{3}$) | $\delta_{IC}^{*}$ (μm) |
|---|---|---|---|---|---|
| AF1410 | | | | | |
| heat 1 | 1528 | 1699 | 1.16 | 0.21 | 28 |
| heat 2 | 1503 | 1659 | 1.16 | 0.23 | 66 |
| heat 3 | 1533 | 1675 | 1.31 | 0.22 | 61 |
| HY180 | | | | | |
| heat 1 | 1208 | 1343 | 1.39 | - | 130 |
| heat 2 | 1236 | 1379 | 1.54 | - | 268 |

*Calculated from $\delta_{IC} = d_n J_{IC}/\sigma_0$ where $\sigma_0$ is the average of the yield and ultimate and $d_n$ are taken from Shih [53] and were 0.60 for AF1410 and 0.67 for HY180.

## Table VII

## Values of $\beta$, $\overline{\delta}_{IC}$ and $\delta'_{IC}$

## for HY180 and AF1410 Steels

## Aged at 510°C*

| Material | f | $\beta(f)$ | $\overline{\delta}_{IC}(f)$ ($\mu$m) | $\delta'_{IC}$ ($\mu$m) |
|---|---|---|---|---|
| HY180 | 0.00018 | 65 | 390 | 890 |
| AF1410 | 0.00038 | 18 | 71 | - |

* Value for $\delta'_{IC}$ is a lower bound.

## Table VIII

## Chemistries of Two Heats of HP9-4-20 Steel[a]

| Material | C | Ni | Co | Mo | Cr | Mn | V | Si | P | S | Ti | Al | $[O]^b_{tot}$ | $[N]^b_{tot}$ |
|---|---|---|---|---|---|---|---|---|---|---|---|---|---|---|
| heat 1 | 0.20 | 9.16 | 4.55 | 1.09 | 0.76 | 0.47 | 0.09 | 0.06 | 0.006 | 0.004 | 0.007 | 0.031 | 11 | 41 |
| heat 2 | 0.21 | 8.57 | 4.27 | 0.94 | 0.77 | 0.26 | 0.09 | 0.04 | 0.005 | 0.002 | 0.004 | 0.009 | 13 | 19 |

[a] wt pct
[b] ppm

## Table IX

## Bulk Inclusion Data for Two Heats of HP9-4-20 Steel

| Microstructure | $R_0$ (μm) | Vol. fraction (f) | $X_0$ (μm) |
|---|---|---|---|
| heat 1 | | | |
| 840°C | 0.25 | .00022* | 3.7 |
| 1050°C | 0.33 | .00016* | 5.4 |
| heat 2 | | | |
| 840°C | 0.17 | 0.00022 | 2.5 |
| 1050°C | 0.20 | 0.00020 | 2.9 |

* Excludes volume fraction of stringers which comprised additional f = 0.00019.

## Table X

## Smooth Axisymmetric Tensile Properties of Two of Heats of HP9-4-20 Steel[a]

| Microstructure | Tensile Strength MPa (Ksi) | Yield Strength MPa (Ksi) | Flow[b] Strength MPa (Ksi) | Pct El. | Pct R.A. | n | $\varepsilon_f^{Axs}$[c] |
|---|---|---|---|---|---|---|---|
| heat 1 | | | | | | | |
| 840°C | 1693 (245.5) | 1272 (184.6) | 1483 (215.0) | 18.8 | 57.5 | 0.14 | 0.86 |
| 1050°C | 1618 (234.6) | 1225 (177.6) | 1421 (206.1) | 17.2 | 56.0 | 0.14 | 0.82 |
| heat 2 | | | | | | | |
| 840°C | 1667 (241.8) | 1154 (167.4) | 1411 (204.6) | 17 | 65.1 | 0.18 | 1.05 |
| 1050°C | 1628 (236.1) | 1122 (162.7) | 1375 (199.4) | 15 | 53.9 | 0.14 | 0.78 |

[a] All results presented are the average of 2 tests

[b] Flow Stress = $\sigma_0 = 1/2(\sigma_Y + \sigma_{UTS})$

[c] $\varepsilon_f^{Axs} = \ln\frac{A_0}{A_f}$

## Table XI

## Fracture Toughness Data for Two Heats of HP9-4-20 Steel

| Microstructure | $J_{IC}$ KJ/m$^2$(in-lb/in$^2$) | $K_{IJ}$[a] MPa$\sqrt{m}$(Ksi$\sqrt{in}$) | $\sigma_0$ MPa (Ksi) | n | $J_{..}$ | $\ldots$ in |
|---|---|---|---|---|---|---|
| heat 1 | | | | | | |
| 840°C | 31.0 (177) | 81.7 (74.5) | 1483 (215 0) | 0 14 | 0 49 | 10 3 |
| 1050°C | 69.2 (395) | 120.9 (111.2) | 1421 (206 1) | 0 14 | 0 49 | 23 5 |
| heat 2 | | | | | | |
| 840°C | 50 (285) | 103.2 (93.9) | 1411 (204.6) | 0.18 | 0 43 | 15 5 |
| 1050°C | 44 (251) | 96.7 (87.0) | 1375 (199.4) | 0.14 | 0.49 | 15 5 |

[a] Calculated from $J_{IC} = K_{IC}^2(1-\nu^2)/E$

Table XII

Summary of Extraction Replica Data

for Two Heats of HP9-4-20 Steel

| | | | | | |
|---|---|---|---|---|---|
| | | | | | |
| | | | | | |
| | | | | | |
| | | | | | |
| | | | | | |
| | | | | | |

## Table XIII

## Compositions of Three Heats of HY180 Steel

## Table XIV

## Mechanical Properties of Three Heats of HY180 Steel Aged at 510°C

| Heat | YS MPa | UTS MPa | $\varepsilon_t$ | n | $J_{IC}$ (MN/m) | $K_{IC}$ (MPa$\sqrt{m}$ | $\delta_{IC}$ (μm) |
|---|---|---|---|---|---|---|---|
| [illegible] | [illegible] | [illegible] | 1.39 | 0.043 | 0.251 | 233 | 129 |
| [illegible] | [illegible] | [illegible] | 1.54 | 0.048 | 0.522 | 336 | 268 |
| [illegible] | [illegible] | [illegible] | 1.58 | 0.044 | 1.375 | 545 | 706 |

## Table XV

## Inclusions in Three Heats of HY180 Steel

| | Type | f | $R_0(\mu m)$ | $X_0(\mu m)$ |
|---|---|---|---|---|
| heat 1 | MnS | 0.00021 | 0.16 | 2.4 |
| heat 2 | $La_2O_2S$ | 0.00015 | 0.44 | 7.5 |
| heat 3 | $Ti_2CS$ | 0.00019 | 0.10 | 1.6 |

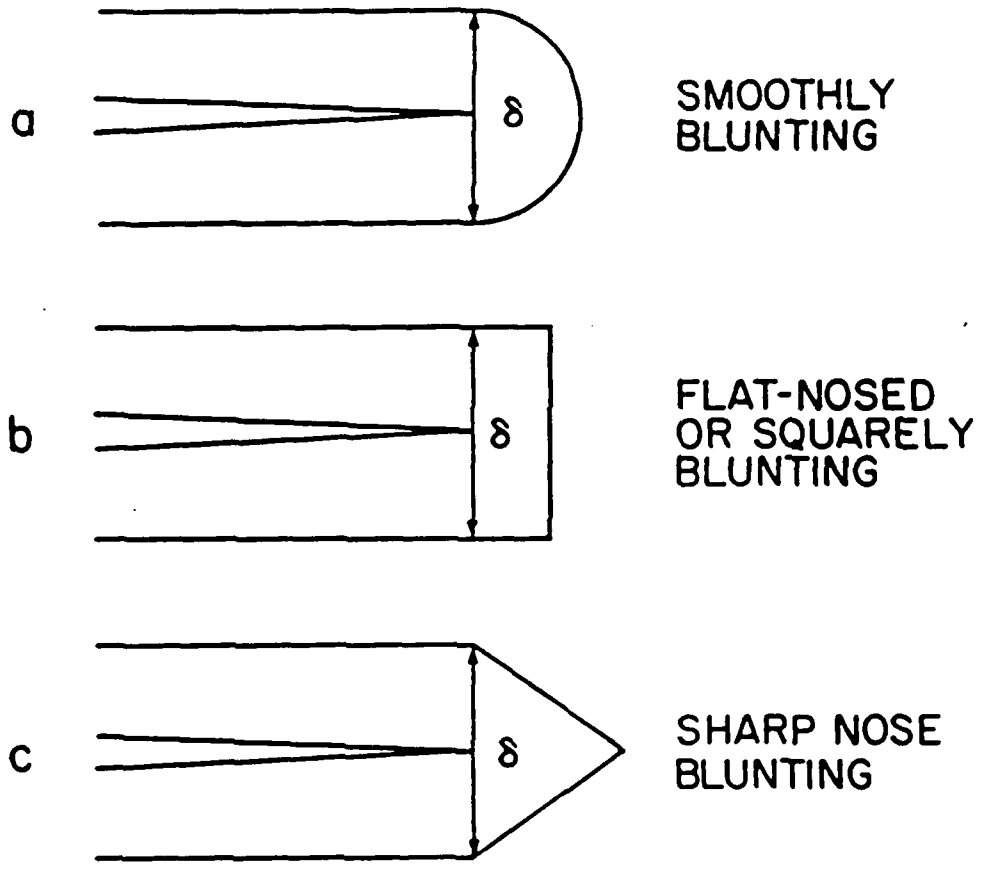


Fig. 1. Illustrations of three blunting geometries. Smooth blunting was assumed by Rice and Johnson [9] in their calculations. Blunting to a flatnose and to a sharp nose are two possible cases of blunting to vertices first suggested by McClintock [18].

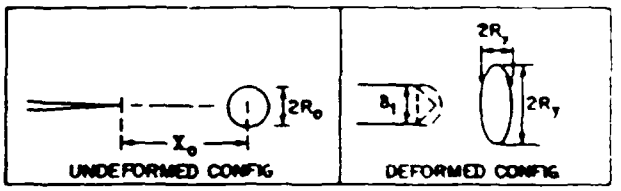


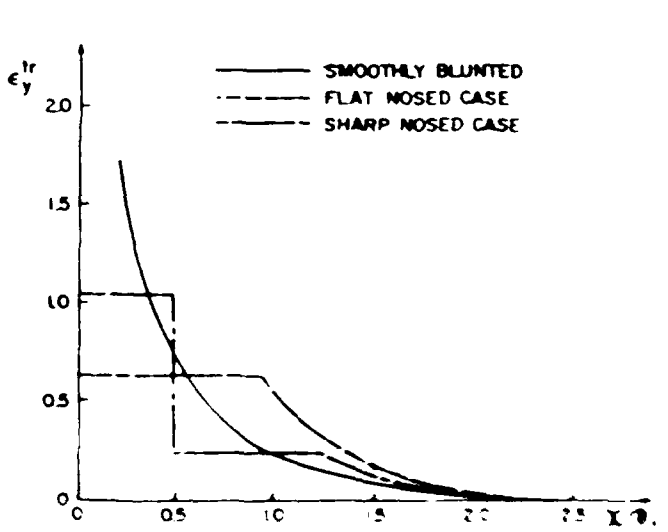


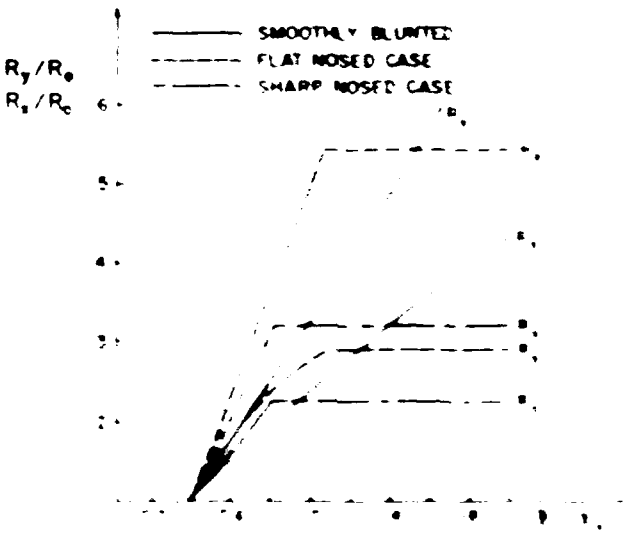


Fig. 2 Results of McMaster[ ] calculations of wall growth for smoothly blunting and blunting flat and sharp noses

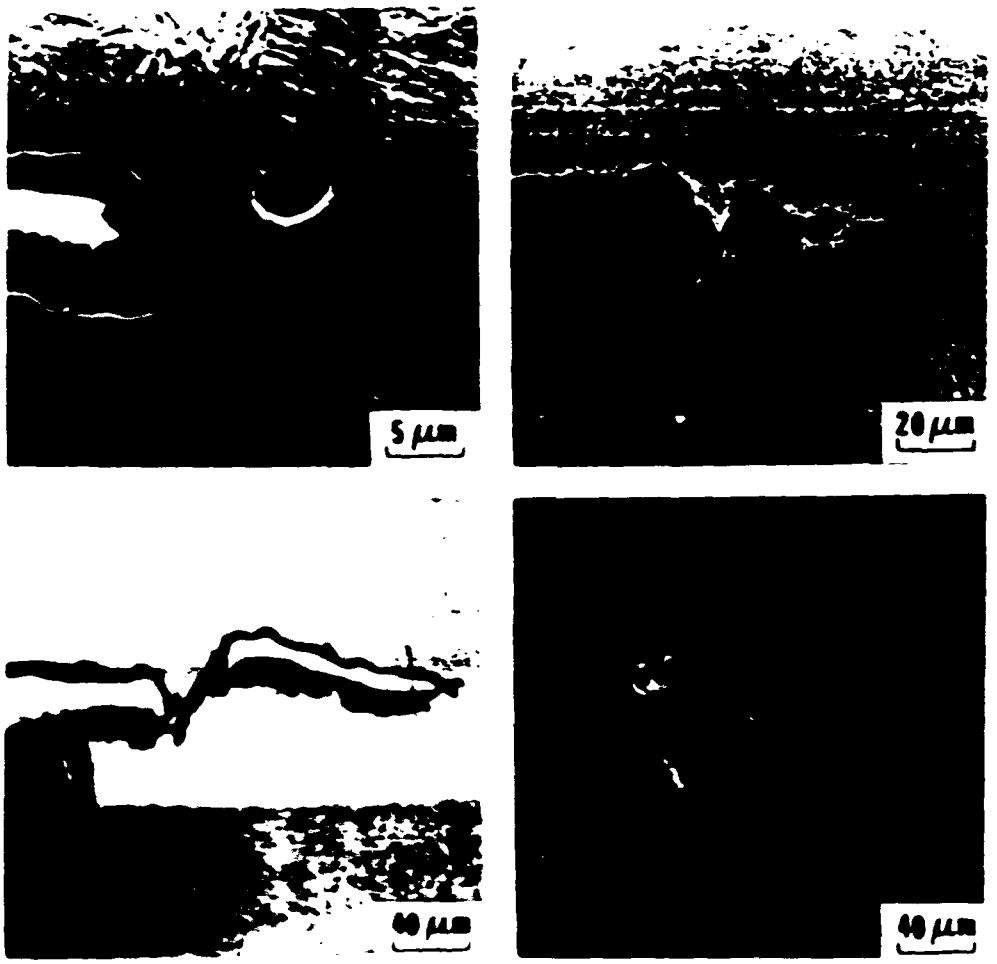


Fig. [illegible] Examples of blunting behaviors observed in HP9-4-20 and HP9-4-10 steels [21]. As-quenched microstructures shown in (a) and (b) for HP9-4-20 and HP9-4-10 respectively exhibit smooth blunting with voids growing just ahead of the blunting crack. The tempered at [illegible] microstructures shown in (c) and (d) for HP9-4-20 and HP9-4-10 respectively, blunt to [illegible]

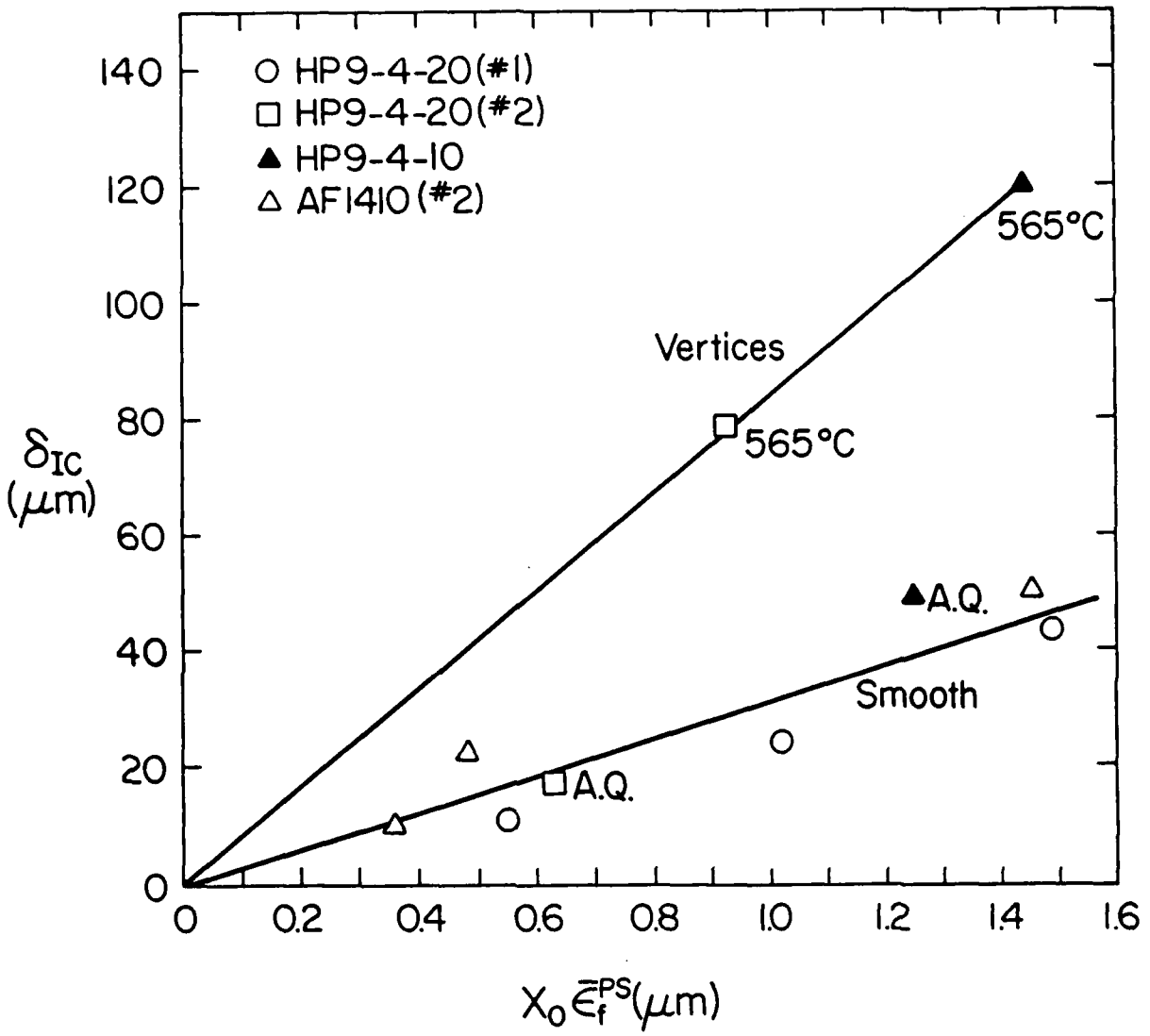


Fig. 4. $\delta_{IC}$ plotted as a function of $X_0\bar{\epsilon}_f^{ps}$ . $\delta_{IC}$ is linear in $X_0\bar{\epsilon}_f^{ps}$ as long as the blunting behavior is a constant. Data are presented only for small inclusion spacings, $X_0$.

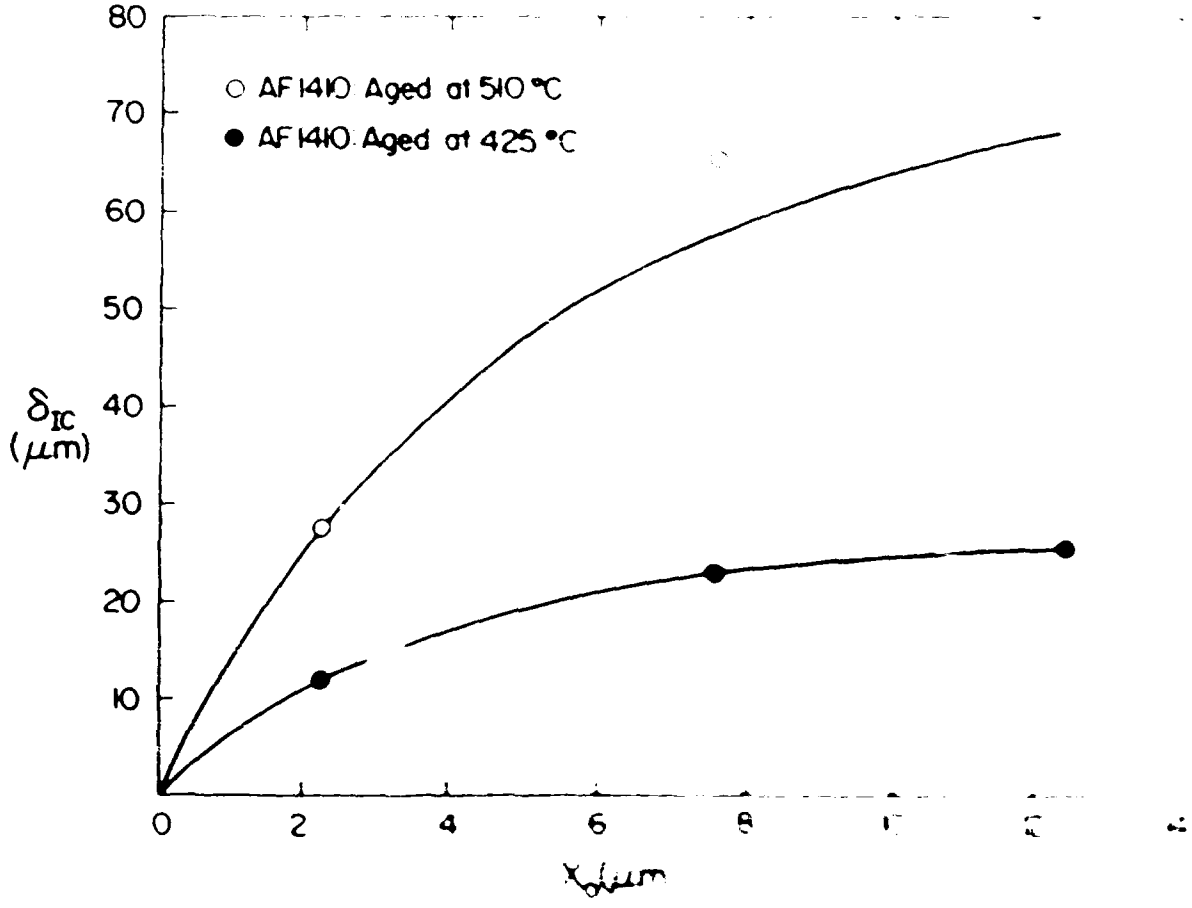


Fig. 5. $\delta_{IC}$ plotted as a function of inclusion spacing, $X_p$, for AF 1410 steel [illegible] C. The inclusion volume fraction is constant [illegible]

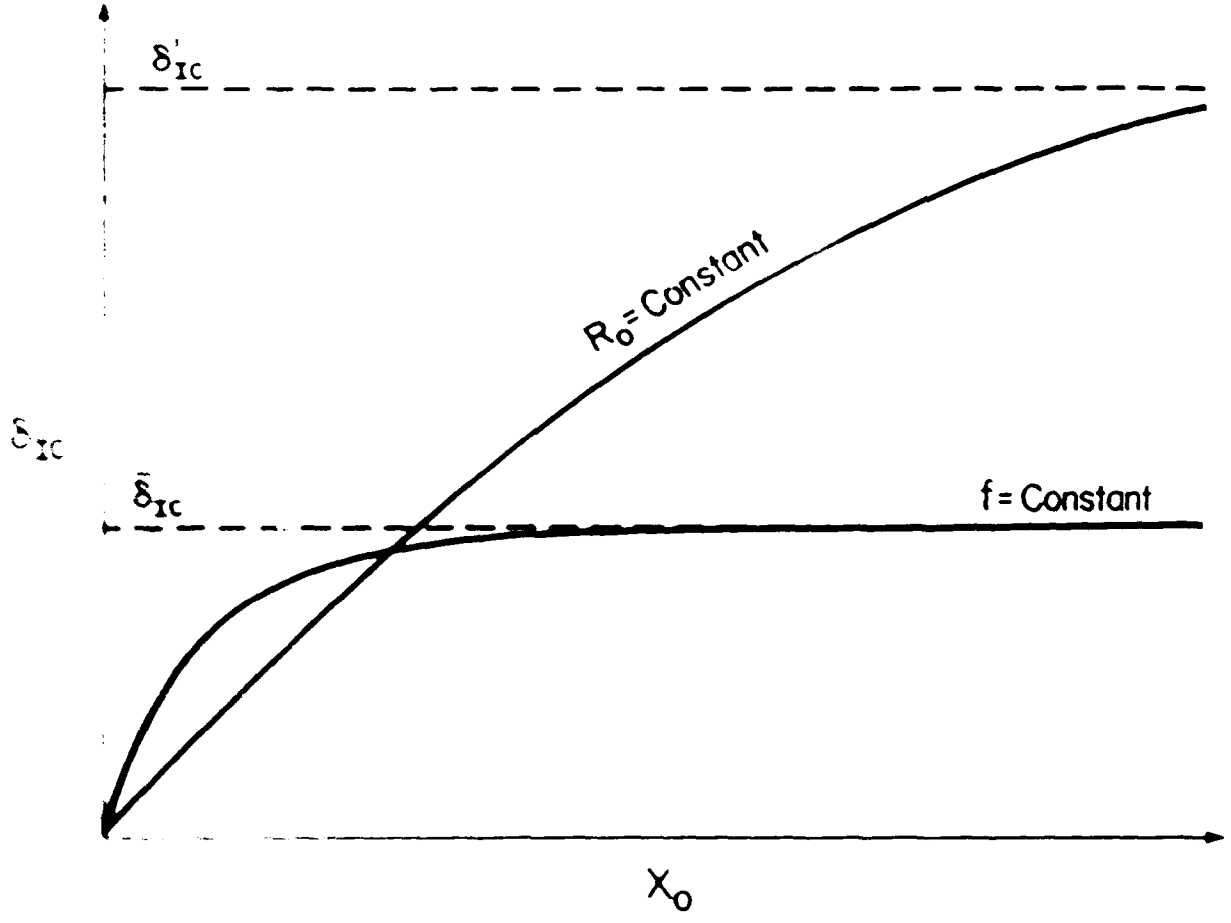


Fig. 4 $\delta_{IC}$ plotted as a function of inclusion spacing. $X_o$ at constant inclusion volume fraction and at constant particle size. As $X_o$ is increased at constant inclusion volume fraction $\delta_{IC}$ approaches a constant, $\bar{\delta}_{IC}$. When $X_o$ is increased at constant particle size $\delta_{IC}$ will approach $\delta'_{IC}$. The magnitude of the difference of inclusions at $X_o$ becomes large

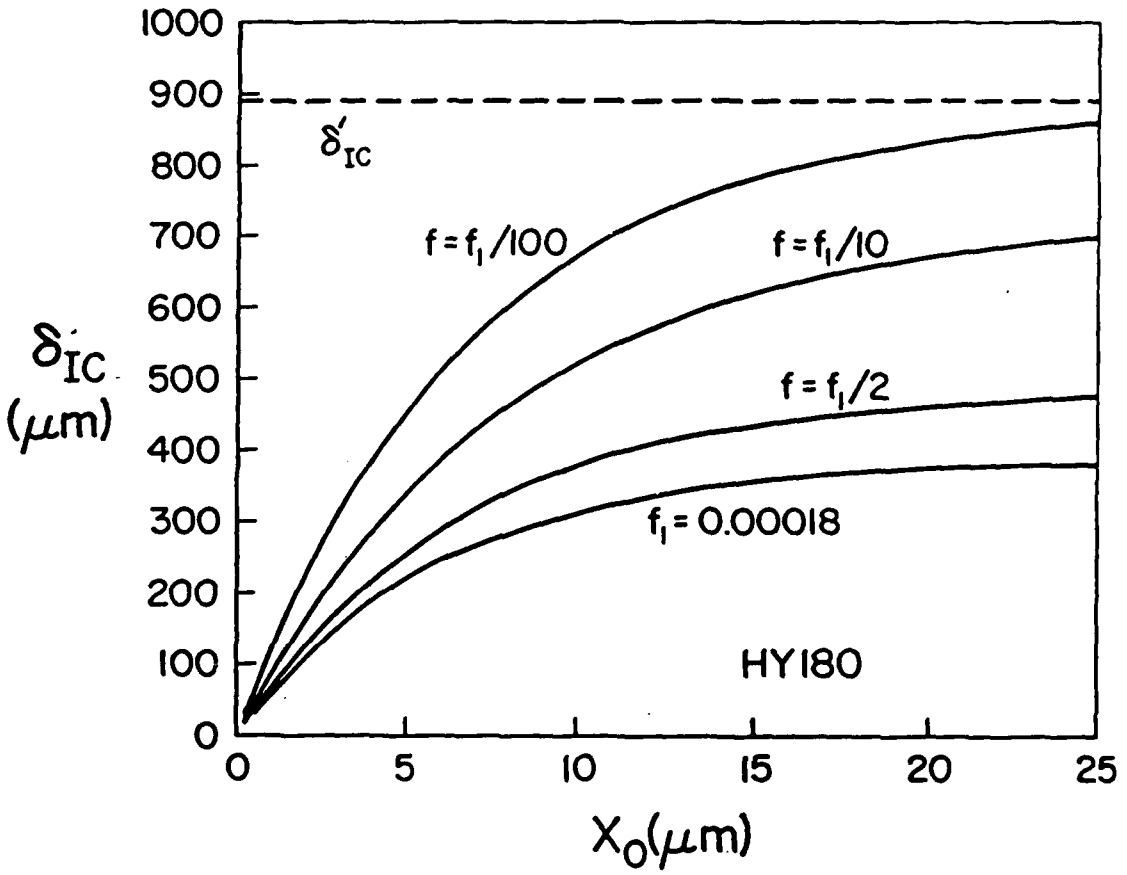


Fig. 7. $\delta_{IC}$ plotted as a function of inclusion spacing, $X_0$ at several inclusion volume fractions for HY180 steel aged at 510°C for 5 hours. Results calculated.

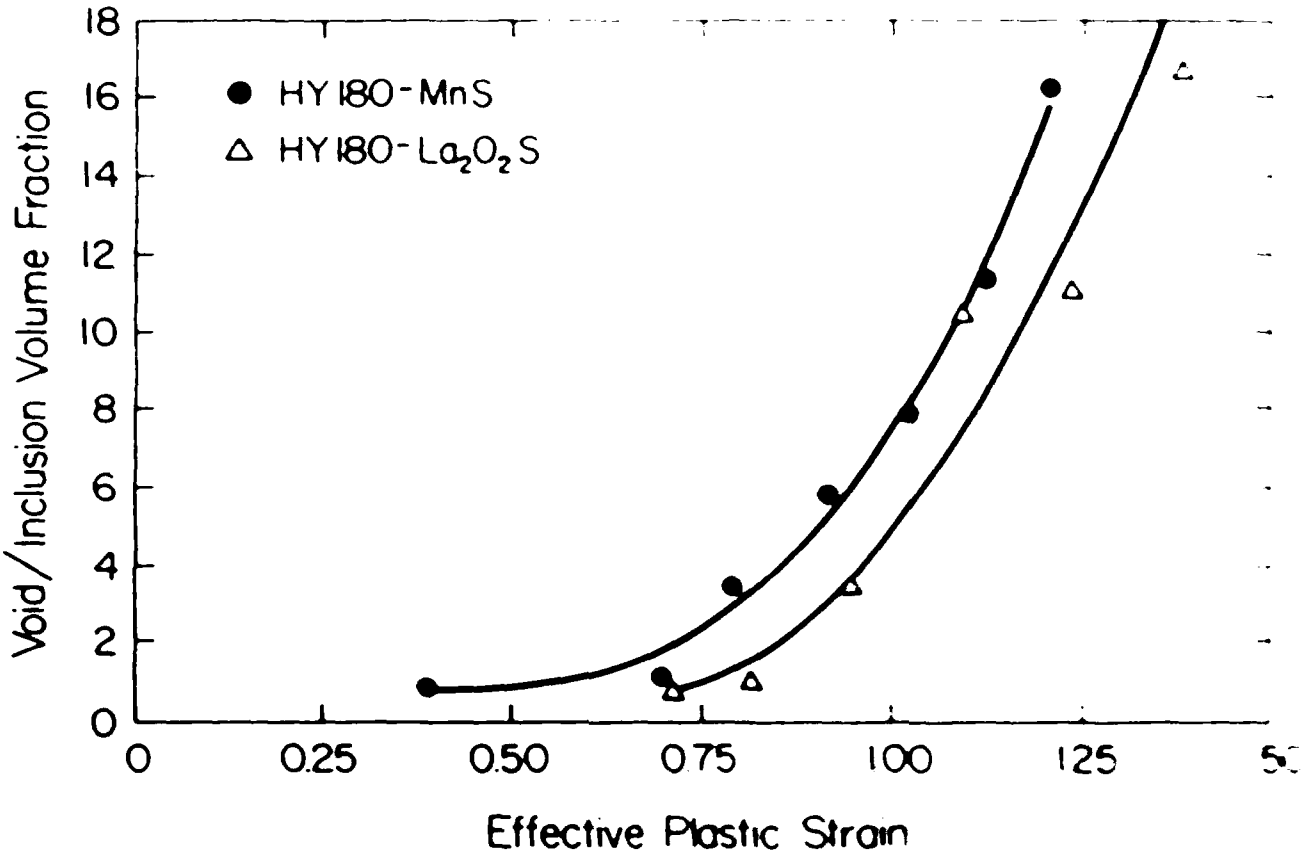


Fig. 8. The void volume fraction normalized by the inclusion volume fraction plotted as a function of strain in uniaxial tension for HY180 steel tempered at 510°C containing either MnS or $La_2O_2S$ inclusions.

WITH SECONDARY PARTICLES

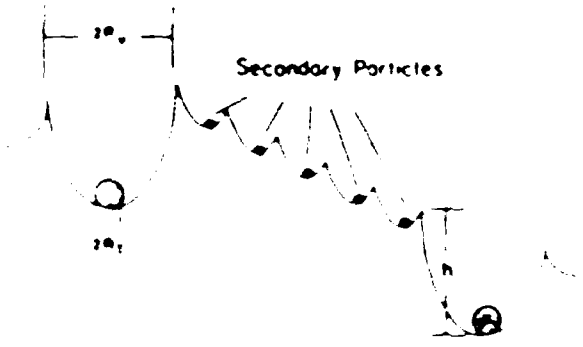


WITHOUT SECONDARY PARTICLES

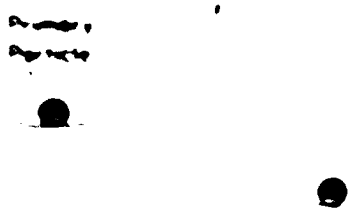

Fig. 5 A schematic of void coalescence by either impingement or by the formation of a void sheet of secondary particles

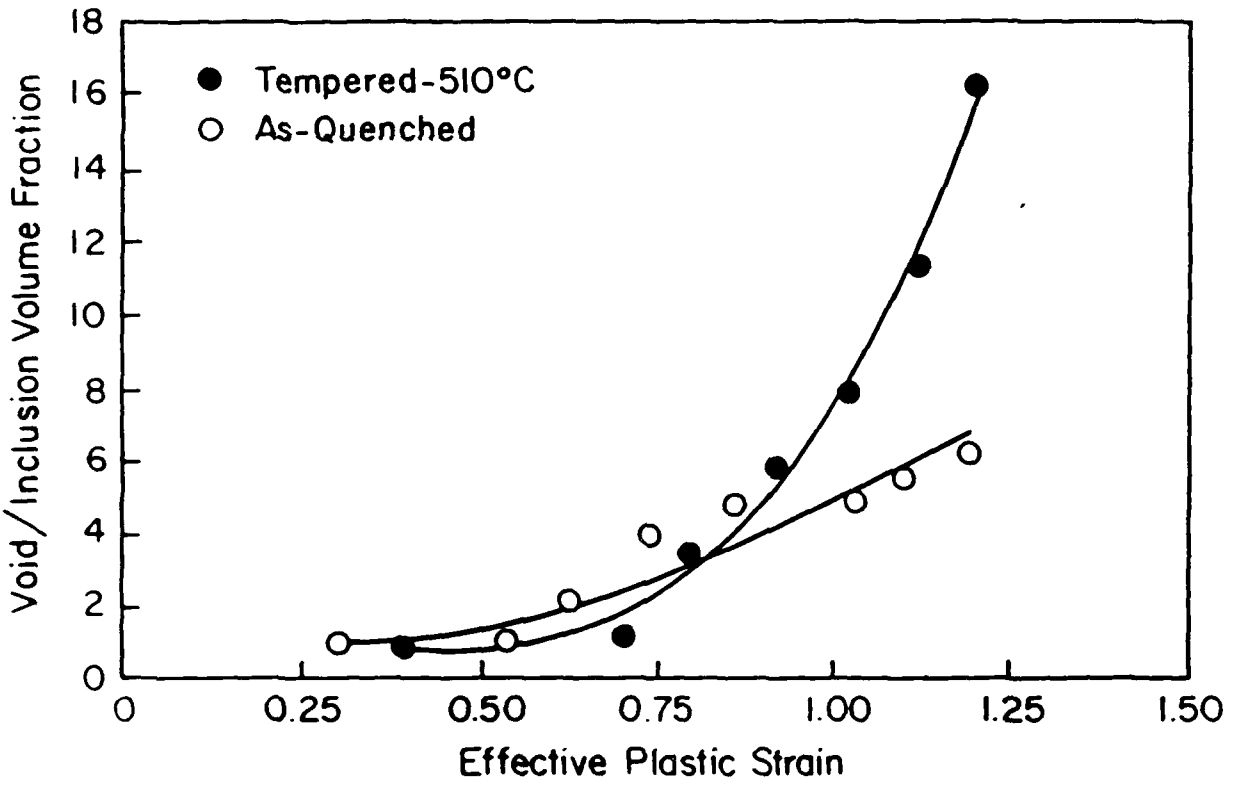


Fig. 10 The void volume fraction normalized by the inclusion volume fraction plotted as a function of strain for the as-quenched and tempered at 510°C microstructures of HY180 steel containing MnS inclusions

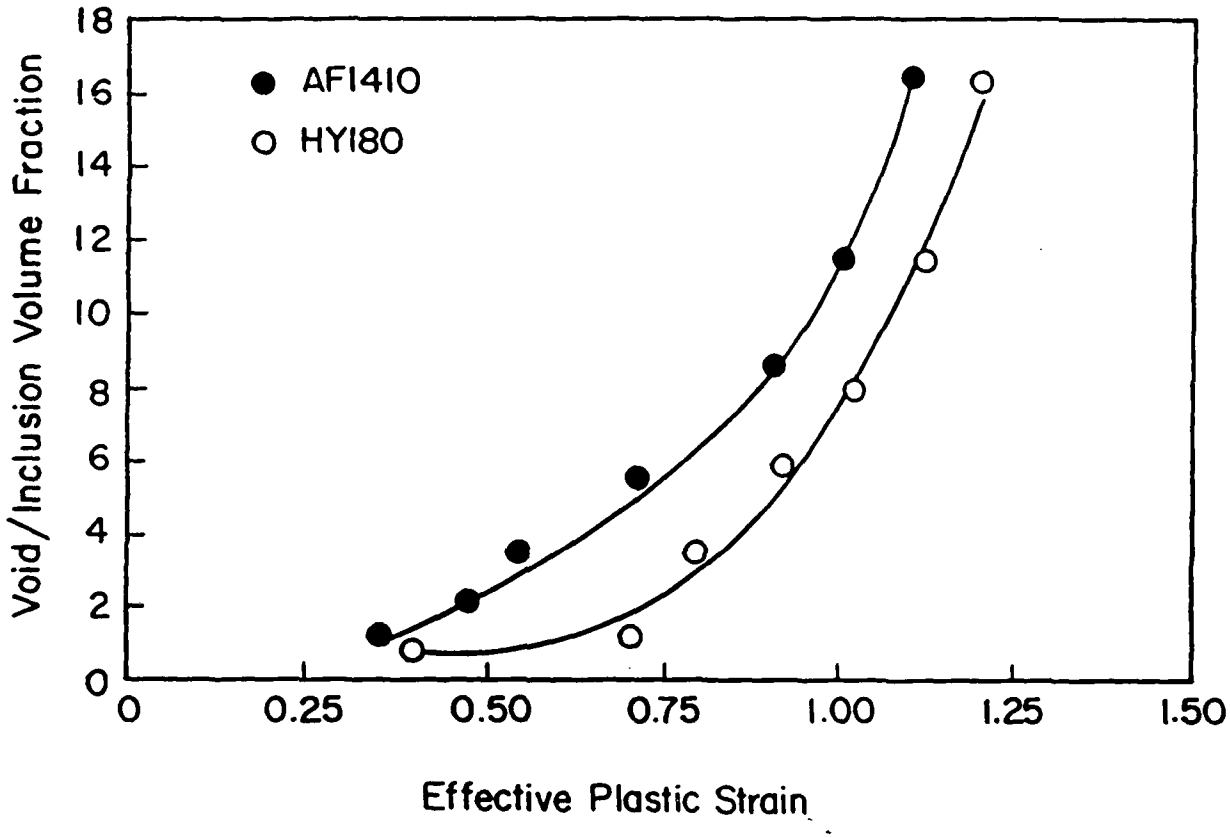


Fig. 11. The void volume fraction normalized by the inclusion volume fraction plotted as a function of strain for the tempered at 510°C microstructures of HY180 steel and AF1410 steel containing MnS inclusions.

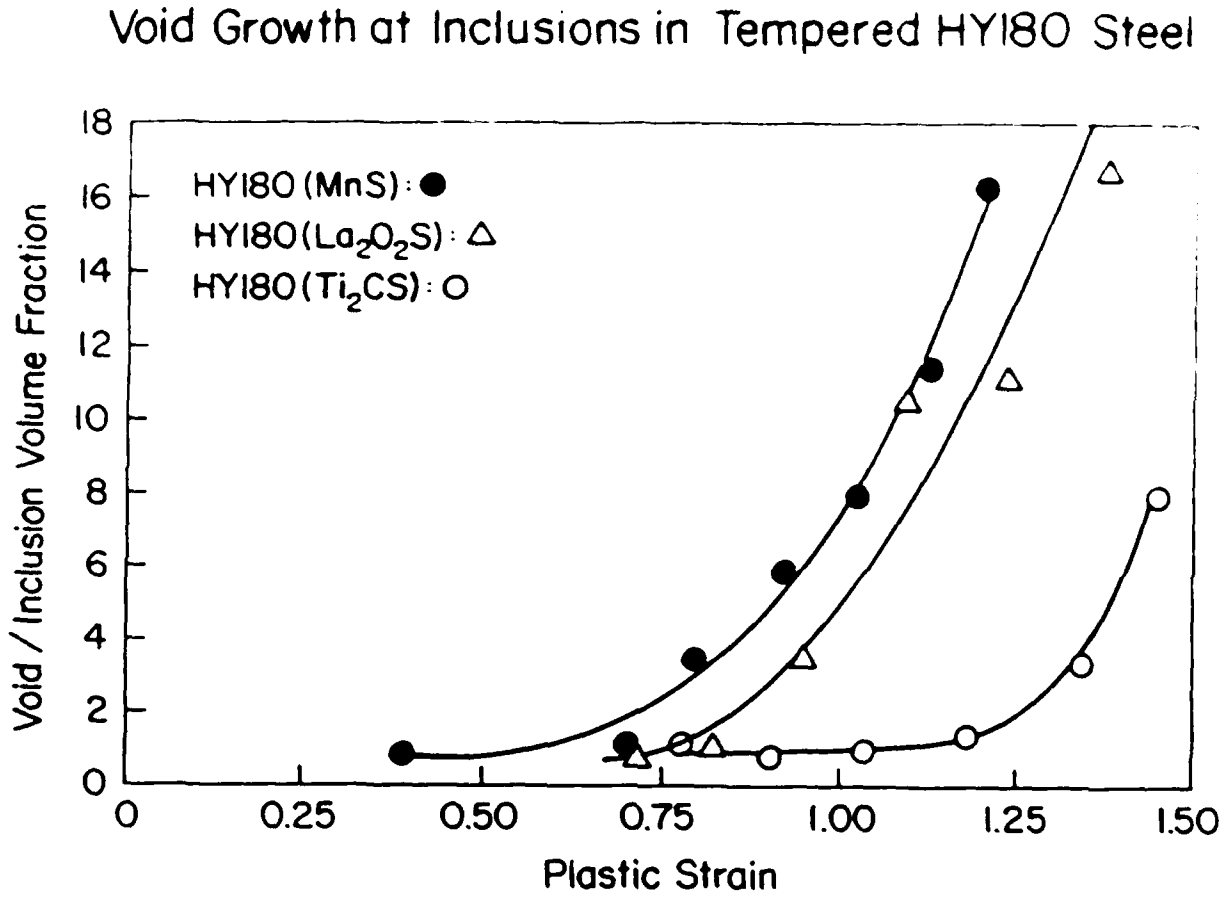


Fig. 12. The void volume fraction normalized by the inclusion volume fraction plotted as a function of strain for the tempered at 510°C microstructure of two heats of HY180 steel containing either MnS or $Ti_2CS$ inclusions (from ref. 14)

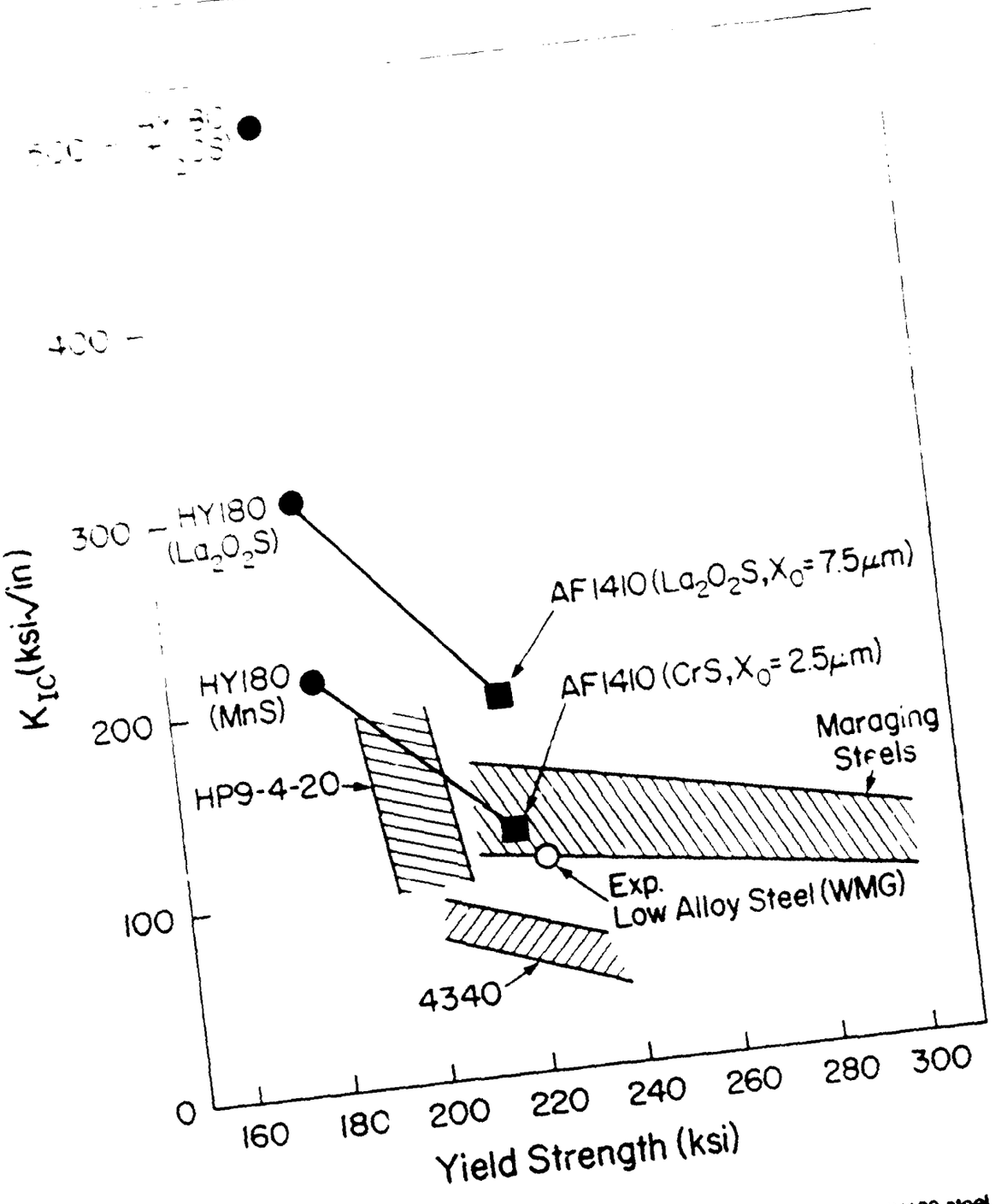


Fig. 13. A plot of fracture toughness ($K_{IC}$) plotted as a function of yield strength. Data for HY180 steel containing MnS ($X_0$ = 2.5 μm), $La_2O_2S$ ($X_0$ = 7.5) and $Ti_2CS$ ($X_0$ = 1.6 μm) inclusions are indicated, as are data for AF1410 containing CrS ($X_0$ = 2.5μm) or $La_2O_2S$ ($X_0$ = 7.5)